JEM Journal of Experimental Medicine

BRIEF DEFINITIVE REPORT

B7 costimulation antagonizes RORγt⁺ regulatory T cells and immune tolerance in the intestine

Mengze Lyu[1,2,3] and Gregory F. Sonnenberg[1,2,3]

Regulatory T (Treg) cells that recognize dietary- or microbiota-derived antigens express RORγt and are essential for immune tolerance in the intestine. A recent paradigm shift found these cells require major histocompatibility complex class II (MHCII) on RORγt⁺ antigen-presenting cells (APCs) rather than conventional dendritic cells (cDCs) for signal one. Here, we evaluate signal two and unexpectedly find that costimulatory molecules B7-1 (CD80) and B7-2 (CD86) antagonize the generation of microbiota-specific RORγt⁺ Treg cells. Gain-of-function or loss-of-function therapeutics targeting B7 via CTLA-4 exert reciprocal effects on the generation of microbiota-specific RORγt⁺ Treg cells. This axis was independent of B7 on RORγt⁺ APCs but required MHCII on this cell type. Finally, CTLA4-Ig treatment restores microbiota-specific RORγt⁺ Treg cell generation and protects from experimental intestinal inflammation induced by pathobiont colonization with IL-10R signaling blockade. These results define that RORγt⁺ Treg cells are uniquely restrained by B7 costimulation, while CTLA4-Ig enhances immune tolerance in the intestine when acting cooperatively with RORγt⁺ APCs.

Introduction

Regulatory T (Treg) cells co-expressing the lineage-defining transcription factors Foxp3 and RORγt represent a specialized subset essential for maintaining immune tolerance within the gastrointestinal tract (Ohnmacht et al., 2015; Sefik et al., 2015; Yang et al., 2016). This unique type of RORγt⁺ Treg cell is peripherally induced, is enriched in the intestinal lamina propria, requires and produces abundant IL-10, and exhibits superior suppressive capabilities over conventional Treg cells. Additionally, RORγt⁺ Treg cells share some overlapping requirements with T helper 17 (T_H17) cells for differentiation, such as IL-6 and IL-23, as well as the presence of gut microbiota (Ohnmacht et al., 2015; Sefik et al., 2015; Yang et al., 2016). Many of these peripherally induced RORγt⁺ Treg cells recognize antigens derived from gut microbiota or dietary cues (Abdel-Gadir et al., 2019; Al Nabhani et al., 2019; Kim et al., 2016; Knoop et al., 2020; Ramanan et al., 2020; Xu et al., 2018), indicating there are key roles and therapeutic relevance for RORγt⁺ Treg cells in states of health, inflammatory bowel disease (IBD), or food allergy.

Understanding the pathways that promote the generation of antigen-specific RORγt⁺ Treg cells has generated considerable interest, with a recent paradigm shift indicating clear distinctions from more conventional Treg cell subsets. This started in part with the discovery of RORγt⁺ antigen-presenting cells (APCs) in the intestine and associated draining lymph nodes of both mice and humans, which were first characterized as lymphoid tissue inducer (LTi)–like group 3 innate lymphoid cells (ILC3s), and experimental deletion of MHCII on RORγt⁺ cells revealed an essential role in restraining inflammatory T cell responses to gut microbiota and preventing intestinal inflammation (Hepworth et al., 2013; Hepworth et al., 2015). With the development of additional models and single-cell RNA-sequencing (scRNA-seq), subsequent studies revealed a family of RORγt⁺ APCs that are necessary and sufficient to instruct the differentiation of microbiota-specific RORγt⁺ Treg cells (Akagbosu et al., 2022; Kedmi et al., 2022; Lyu et al., 2022; Wang et al., 2021; Yamano et al., 2019). Strikingly, and in contrast to conventional Treg cells, the generation of antigen-specific RORγt⁺ Treg cells occurred independently of MHCII on cDCs (Akagbosu et al., 2022; Kedmi et al., 2022; Lyu et al., 2022). There are also critical roles for RORγt⁺ APCs in establishing oral tolerance to dietary antigens via RORγt⁺ Treg cell differentiation and by restraining allergen-specific T helper 2 cell responses (Cabric et al., 2025; Fu et al., 2025; Narasimhan et al., 2025; Rodrigues et al., 2025; Sun et al., 2025; Teng et al., 2021), or impacting other diverse immune responses in neuroinflammation, colon cancer, or following fungal infection (Dobes et al., 2022; Goc et al., 2021; Grigg et al., 2021). Importantly, there is evidence of altered RORγt⁺ Treg cells and RORγt⁺ APCs in the inflamed intestine of IBD patients or food allergy patients (Abdel-Gadir et al., 2019; Hepworth et al., 2015;

[1]Joan and Sanford I. Weill Department of Medicine, Division of Gastroenterology & Hepatology, Weill Cornell Medicine, Cornell University, New York, NY, USA; [2]Department of Microbiology & Immunology, Weill Cornell Medicine, Cornell University, New York, NY, USA; [3]Jill Roberts Institute for Research in Inflammatory Bowel Disease, Weill Cornell Medicine, Cornell University, New York, NY, USA.

Correspondence to Gregory F. Sonnenberg: gfsonnenberg@med.cornell.edu; Mengze Lyu: mel4003@med.cornell.edu.

Lyu et al., 2022), indicating that these cell types support immune tolerance and gut health in humans.

These collective studies demonstrate the necessity of RORγt⁺ APCs in the generation of RORγt⁺ Treg cells via MHCII or signal one, but the requirements for signal two remain poorly defined. CD80 and CD86 (or B7 costimulation) are expressed on professional APCs and are pivotal in the activation of naïve T cells by engaging CD28 (Azuma et al., 1993; Burke et al., 2024; Caux et al., 1994; Freeman et al., 1993; Green et al., 1994; Lenschow et al., 1996; Linsley and Ledbetter, 1993; Sharpe and Freeman, 2002). CTLA-4, another counter-receptor for B7 molecules on T cells and enriched on Treg cells, acts as a critical negative regulator, maintaining immune homeostasis by attenuating T cell responses (Leach et al., 1996; Tivol et al., 1995; Wing et al., 2008). Together with antigen engagement by the T cell receptor (TCR) binding to MHCII with a cognate peptide, CD28 binds to B7 and generates a synergistic signal that activates PI3K and subsequently phosphorylates Akt to drive T cell survival and proliferation (Appleman et al., 2002; Barata et al., 2004). Beyond PI3K-Akt, CD28 engagement also activates NF-κB, MAPK, and mTOR pathways, reinforcing IL-2 transcription, metabolic reprogramming, and sustained effector differentiation (Acuto and Michel, 2003; Chi, 2012; Esensten et al., 2016; Zhang et al., 1999). While it has long been acknowledged that conventional and thymic-derived Treg cells require B7 engagement of CD28 costimulatory signaling (Salomon et al., 2000; Tang et al., 2003), the role of this pathway in the development of RORγt⁺ Treg cells remains unexplored and should be considered given the unique requirements of this subset.

Here, we demonstrate that CD28 activation through CD80 and CD86 engagement unexpectedly antagonizes antigen-specific RORγt⁺ Treg cells in the gut. This could be driven by blocking CD80 and CD86 with CTLA4-Ig, also known as Abatacept, which is an FDA-approved drug for treating multiple human inflammatory or autoimmune diseases (Moreland et al., 2006). Surprisingly, generation of microbiota-specific RORγt⁺ Treg cells was not impacted by B7 on RORγt⁺ APCs, whereas CTLA4-Ig–mediated expansion required MHCII on these APCs. Further, in a mouse colitis model of *Helicobacter hepaticus* (Hh) colonization combined with anti-IL-10R blockade that recapitulates microbiota-driven gut inflammation and features of human IBD (Kullberg et al., 1998; Kullberg et al., 2001; Kullberg et al., 2006), we demonstrate that blocking B7 costimulation enhances RORγt⁺ Treg cell generation to provide striking protection, but only in the presence of signal one from RORγt⁺ APCs, provoking a new strategy to drive effective immune tolerance in the gut.

Results and discussion

B7 costimulation antagonizes microbiota-specific RORγt⁺ Treg cells in the gut

To investigate the role of costimulation on RORγt⁺ Treg cell responses in the gut, we utilized a previously established model to track the development of antigen-specific T cell responses to Hh colonization in the intestines of wild-type (WT) C57BL/6J mice (Xu et al., 2018). In brief, congenically marked naïve CD4 T cells from Hh-specific TCR transgenic (HH7-2tg) mice were adoptively transferred into Hh-colonized recipients with or without B7 costimulation blockade. Two weeks after transfer, we analyzed Hh-specific T cells in the mesenteric lymph nodes (mLNs) and large intestine (LI) (Fig. S1 A). As expected, Hh-specific T cells efficiently differentiated into RORγt⁺ Treg cells in control mice, but surprisingly, this was significantly enhanced in mice treated with anti-CD80 and anti-CD86 blocking antibodies (Fig. 1, A–C). The administration of blocking antibodies had a minor effect on the endogenous RORγt⁺ Treg cell population in the mLN and LI of the recipients (Fig. S1, B and C). We next assessed CD80 and CD86 knockout mice (Borriello et al., 1997) relative to littermates that were complemented with a floxed CD80 transgene (CD80/86KO; CD80Tg$^{fl/fl}$), which rescues B7 expression and permits deletion in a lineage-specific manner (Watanabe et al., 2017). Consistent with our antibody blockade studies, mice with a complete knockout of CD80 and CD86 exhibited significantly expanded Hh-specific and endogenous RORγt⁺ Treg cells in both mLN and LI relative to littermates that were complemented to restore CD80 expression in all cell types (Fig. 1, D–I). In contrast, endogenous RORγt⁻ conventional Treg cells were significantly decreased in CD80 and CD86 knockout mice (Fig. S1 D), which is consistent with previous reports (Salomon et al., 2000; Tang et al., 2003). Given the critical role of RORγt⁺ APCs in instructing RORγt⁺ Treg cells via signal one (Akagbosu et al., 2022; Kedmi et al., 2022; Lyu et al., 2022), we investigated whether conditional deletion of B7 in RORγt⁺ APCs impacts RORγt⁺ Treg cell induction by crossing the above mice with RORγt^{Cre} mice. In this context, we found no significant impact on Hh-specific and endogenous RORγt⁺ Treg cells in both mLN and LI (Fig. 1, D–I). In addition, we examined RORγt⁻ conventional Treg cells in these mice and observed no changes (Fig. S1 D). Collectively, these findings identify that in contrast to conventional Treg cells, the generation of RORγt⁺ Treg cells does not require B7 costimulation, and rather, B7 costimulation on cell types other than RORγt⁺ APCs antagonizes the development of RORγt⁺ Treg cells.

Therapeutics targeting CTLA-4 can be harnessed to modulate RORγt⁺ Treg cells

CTLA-4 has a greater affinity for CD80 and CD86 than CD28, thus permitting a block in activation of T cells (Collins et al., 2002; Schwartz et al., 2001; Stamper et al., 2001). Therefore, we next examined the impact of CD80 and CD86 blockade on Hh-specific RORγt⁺ Treg cell generation by harnessing the CTLA4-Ig fusion protein (Fig. S1 E), an FDA-approved molecule that is used in autoimmune conditions but failed to demonstrate efficacy in IBD patients (Davenport et al., 2002; Kremer et al., 2003; Kremer et al., 2005; Kremer et al., 2006; Linsley et al., 1991; Moreland et al., 2006; Read et al., 2000; Ruperto et al., 2008; Sandborn et al., 2012). Consistent with the results obtained with B7 costimulatory blocking antibodies, mice treated with CTLA4-Ig exhibited a significantly increased Hh-specific RORγt⁺ Treg cell population, accompanied by a significant increase in the endogenous RORγt⁺/RORγt⁻ Treg cell ratio in the mLN and LI relative to those treated with the isotype control antibody (Fig. 2, A–C; and Fig. S1, F and G). Thus, it is possible to harness a gain-of-function

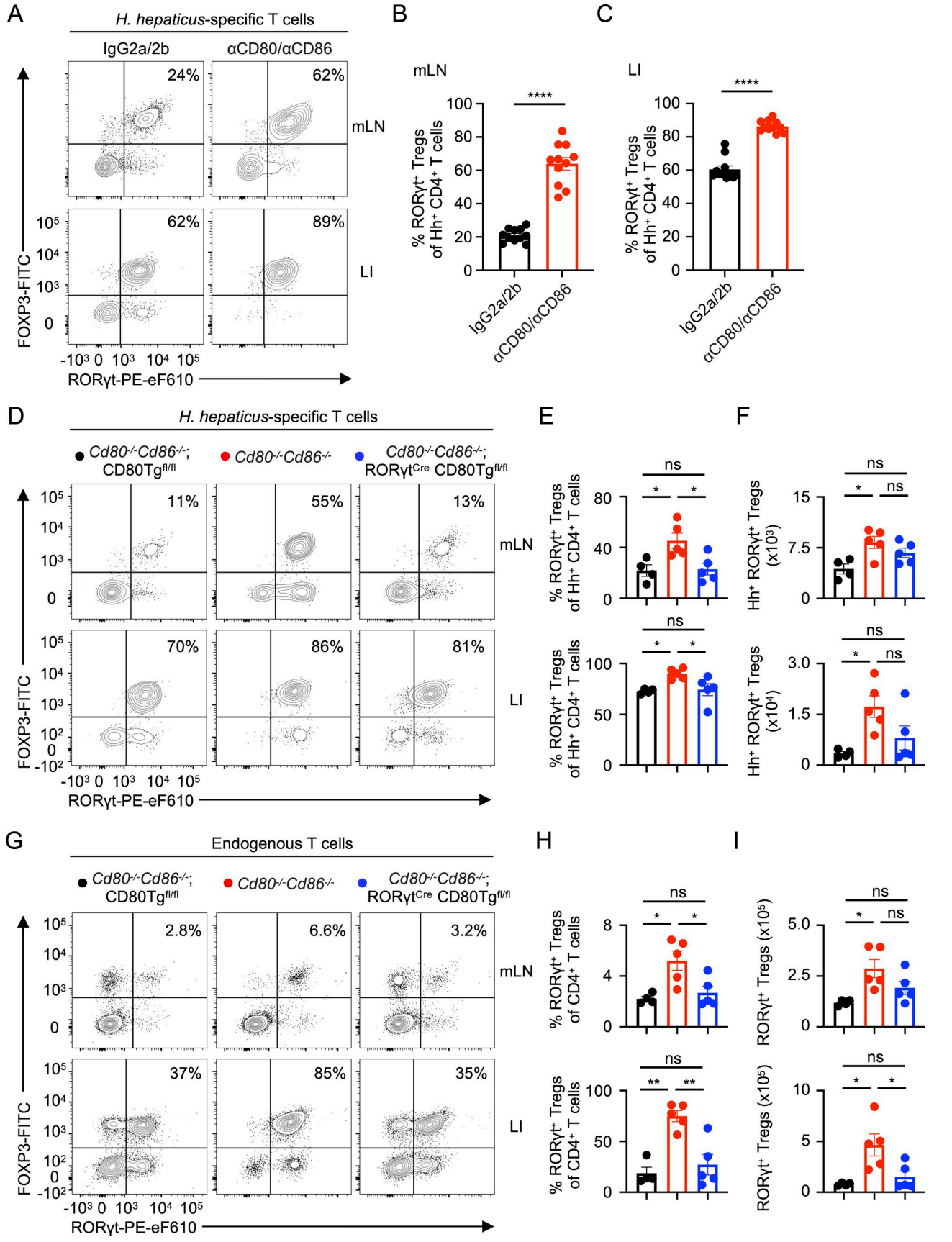

Figure 1. **B7 costimulation antagonizes RORγt⁺ Treg cell responses in the gut. (A–C)** (A) Flow cytometry plots of Hh-specific CD4⁺ T cells (mLN, top panel; LI, bottom panel) and frequency of RORγt⁺ Treg cells in the (B) mLN and (C) LI of C57BL/6J WT mice treated with IgG2a/2b (n = 11) or αCD80/αCD86 (n = 11).

RORγt⁺ Treg cells were gated as CD4⁺ Foxp3⁺ RORγt⁺ T cells, and this strategy was applied consistently in all experiments. **(D–F)** (D) Flow cytometry plots, (E) frequency, and (F) cell number of Hh-specific RORγt⁺ Treg cells in the mLN (top panel) and LI (bottom panel) of *Cd80*$^{-/-}$*Cd86*$^{-/-}$; CD80Tg$^{fl/fl}$ mice (n = 4), *Cd80*$^{-/-}$*Cd86*$^{-/-}$ mice (n = 5), and RORγt^{Cre} *Cd80*$^{-/-}$*Cd86*$^{-/-}$; CD80Tg$^{fl/fl}$ mice (n = 5). **(G–I)** (G) Flow cytometry plots, (H) frequency, and (I) cell number of endogenous RORγt⁺ Treg cells in the mLN (top panel) and LI (bottom panel) of *Cd80*$^{-/-}$*Cd86*$^{-/-}$; CD80Tg$^{fl/fl}$ mice (n = 4), *Cd80*$^{-/-}$*Cd86*$^{-/-}$ mice (n = 5), and RORγt^{Cre} *Cd80*$^{-/-}$*Cd86*$^{-/-}$; CD80Tg$^{fl/fl}$ mice (n = 5). The data in Fig. 1 are pooled from three independent experiments. The data are shown as means ± SEM; the statistics shown in E, F, H, and I were obtained by ordinary one-way ANOVA with Tukey's multiple comparisons test. ns, not significant; *P < 0.05; **P < 0.01; ****P < 0.0001.

CTLA-4 therapeutic to boost the abundance of RORγt⁺ Treg cells in the gut.

To examine cellular pathways involved in the effect of CTLA4-Ig on the RORγt⁺ Treg cells, we isolated cells from the mLN and LI of C57BL/6J mice and detected robust binding of CTLA4-Ig to cDCs and macrophages (Fig. S2, A–D). To distinguish subsets within RORγt⁺ APCs, we developed a refined gating strategy informed by our previously published scRNA-

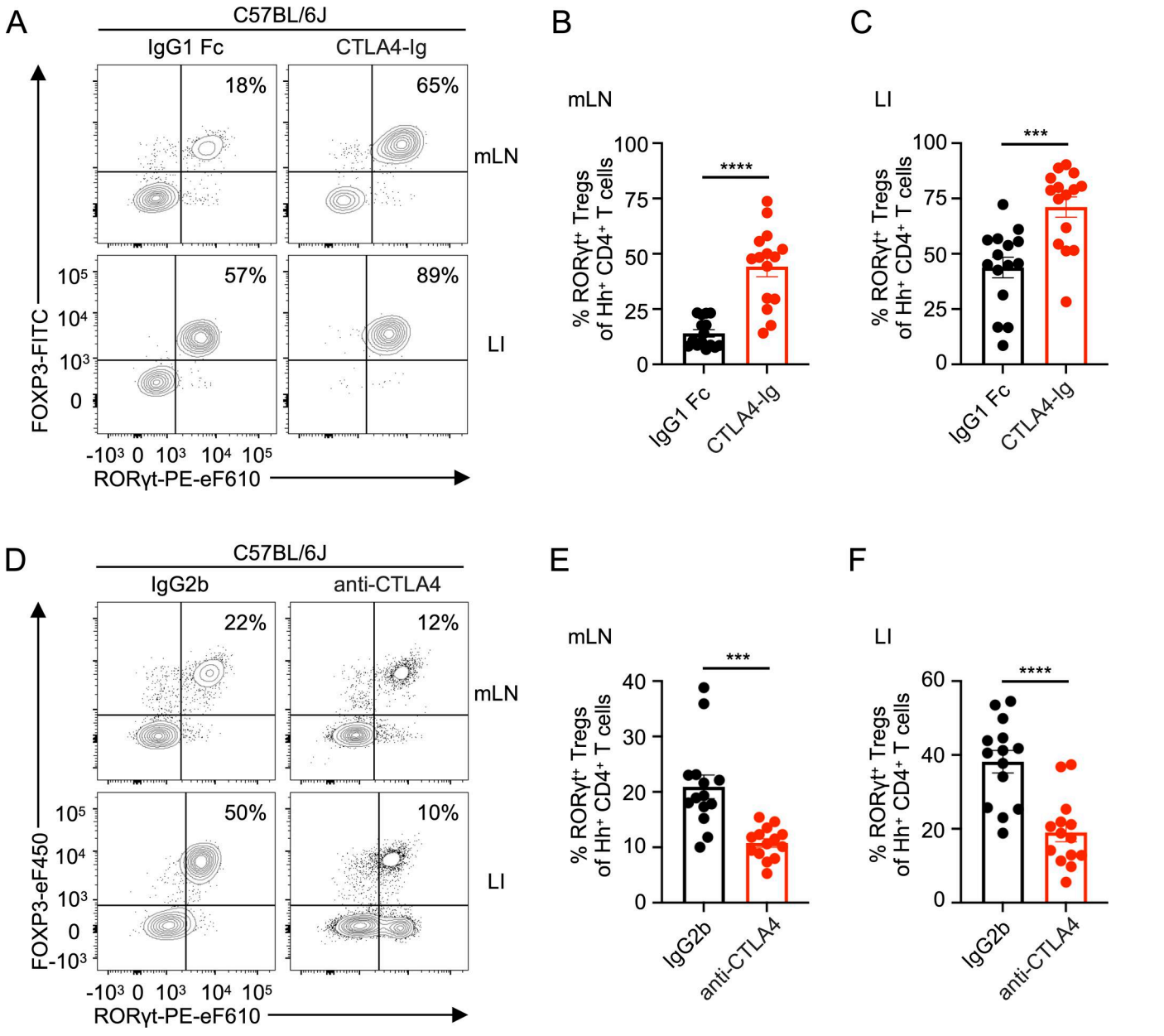

Figure 2. **CTLA-4 modulation engages B7-dependent regulation of RORγt⁺ Treg cells. (A–C)** (A) Flow cytometry plots of the Hh-specific CD4⁺ T cells (mLN, top panel; LI, bottom panel) and frequency of RORγt⁺ Treg cells in the (B) mLN and (C) LI of Hh-colonized WT mice treated with IgG1 Fc (n = 15) or CTLA4-Ig (n = 15). **(D–F)** (D) Flow cytometry plots of the Hh-specific CD4⁺ T cells (mLN, top panel; LI, bottom panel) and frequency of RORγt⁺ Treg cells in the (E) mLN and (F) LI of Hh-colonized WT mice treated with IgG2b (n = 14) or anti-CTLA4 (n = 14). The data in Fig. 2 are pooled from three independent experiments. The data are shown as means ± SEM; the statistics shown in B, C, E, and F were obtained by unpaired two-tailed Student's t test. ***P < 0.001; ****P < 0.0001.

seq data from healthy mouse mLNs (Lyu et al., 2022), based on the mutually exclusive expression of *Klrb1b* and *Spi1*, enabling discrimination of ILC3s and extrathymic AIRE-expressing cells (eTACs), respectively (Fig. S2 A). Using this approach, CTLA4-Ig binding was observed on RORγt$^+$ APCs in the mLN and LI, with a particular enrichment in eTACs within the mLN, while minimal CTLA4-Ig binding was observed on T cells (Fig. S2, B–D). We next examined how CTLA4-Ig treatment changes the frequency and number of each of these APC populations. We observed that CTLA4-Ig treatment decreased the numbers of cDCs and macrophages in the LI, but not in the mLN (Fig. S2, E and F). In addition, CTLA4-Ig treatment increased the frequency of RORγt$^+$ APCs in the mLN and LI, and increased their absolute number in the LI, providing an expanded pool of RORγt$^+$ APCs that may support RORγt$^+$ Treg cell differentiation (Fig. S2, E and F), which is likely through signal one they provide (Akagbosu et al., 2022; Kedmi et al., 2022; Lyu et al., 2022), as CD80 expression on RORγt$^+$ APCs did not impact endogenous or Hh-specific RORγt$^+$ Treg cell responses compared with those in littermate control mice (Fig. 1, D–I). Moreover, we examined CD80 and CD86 levels on these APC subsets following *in vivo* CTLA4-Ig treatment, and found significantly increased CD80 and CD86 levels on macrophages and RORγt$^+$ APCs in the mLN but significantly decreased CD80 and CD86 levels on RORγt$^+$ APCs in the LI, with no detectable changes in other populations from either tissue (Fig. S2, E and F).

To determine whether B7 costimulation provided by cDCs is responsible for the suppression of RORγt$^+$ Treg cells, we generated mice with conditional deletion of CD80 in cDCs by crossing *Clec9a*^{Cre} mice with CD80/86KO; CD80Tg$^{fl/fl}$ mice. However, we did not observe changes in Hh-specific or endogenous RORγt$^+$ Treg cells (Fig. S1, H and I), nor did we see a change in RORγt$^-$ conventional Treg cells in the mLN and LI (Fig. S1, J and K). These data suggest that CD80 on cDCs is at least not solely responsible for the suppressive effect on RORγt$^+$ Treg cells and rather that other specific APC subsets act dominantly or redundantly in regulating this cellular program.

Collectively, these data indicate that CTLA4-Ig acts primarily by binding to B7 on multiple types of APCs, which then promotes RORγt$^+$ Treg cell generation primarily through inhibiting the engagement of CD28 signaling. In support of this conclusion, we pursued a loss-of-function approach by blocking CTLA-4 with an antibody (Fig. S1 E) and observed a significant reduction in the generation of Hh-specific RORγt$^+$ Treg cells in the mLN and LI of mice relative to those treated with the isotype control antibody (Fig. 2, D–F).

CTLA4-Ig enforces RORγt$^+$ Treg cells and protects from experimental gut inflammation

Treg cells are impaired in the context of IL-10R deficiency, a common mutation occurring in very-early-onset IBD patients (Glocker et al., 2009; Kelsen et al., 2015). Further, RORγt$^+$ Treg cells have been identified as a key mediator of antigen-specific immune tolerance to commensal microbiota in the intestine and as a critical suppressor of colitis (Ohnmacht et al., 2015; Sefik et al., 2015; Yang et al., 2016). Therefore, we next sought to determine whether CTLA4-Ig administration impacts RORγt$^+$ Treg cell generation or provides protection in a mouse colitis model induced following Hh colonization combined with IL-10R blockade (anti-IL-10R) (Fig. 3 A). In particular, Hh colonization combined with IL-10 deficiency prevents the differentiation of Hh-specific RORγt$^+$ Treg cells and rather drives the expansion of Hh-specific effector T cells that promote intestinal inflammation (Xu et al., 2018). Strikingly, in this context, CTLA4-Ig administration overcomes a block in RORγt$^+$ Treg cell generation, dramatically expanding Hh-specific RORγt$^+$ Treg cells and reducing Hh-specific T_H17 cells in both the mLN and LI relative to mice treated with the IgG1 Fc control (Fig. 3, B–D). Consistent with previous studies demonstrating that the transcription factor c-Maf is critical for RORγt$^+$ Treg cell differentiation (Wheaton et al., 2017; Xu et al., 2018), we observed that the expression of c-Maf was significantly upregulated in Hh-specific T cells of mice treated with CTLA4-Ig compared with IgG1 Fc (Fig. S3, A and B). Moreover, in CTLA4-Ig–treated mice, Hh-specific T cells significantly downregulated T-bet and produced significantly less interferon-γ (IFNγ) and tumor necrosis factor (TNF) relative to controls (Fig. 3, E–H). Importantly, CTLA4-Ig administration significantly ameliorated parameters of intestinal inflammation, including typhlocolitis, enlarged mLNs, inflammation-associated pathology, and neutrophil infiltration in the LI (Fig. 3, I–L). Beyond antigen-specific T cell responses, CTLA4-Ig–treated mice exhibited a marked increase in endogenous RORγt$^+$ Treg cells, elevated c-Maf levels, and a concurrent reduction in T_H17 cells (Fig. S3, C–G). These endogenous T_H17 cells displayed a reduced pro-inflammatory phenotype, characterized by diminished T-bet expression and reduced production of IFNγ, TNF, and IFNγ$^+$IL-17A$^+$ coproducing cells (Fig. S3, H–M). These findings demonstrate that CTLA4-Ig treatment is sufficient to overcome a block in microbiota-specific RORγt$^+$ Treg cell generation due to a deficiency in IL-10R signaling, as well as provide significant protection from gut inflammation.

RORγt$^+$ APCs are necessary for CTLA4-Ig–driven immune tolerance in the gut

CTLA4-Ig, also known as abatacept or Orencia, was tested in treating multiple human inflammatory or autoimmune diseases such as rheumatoid arthritis, psoriatic arthritis, type 1 diabetes, multiple sclerosis, alopecia totalis, systemic lupus erythematosus, and IBD (Kremer et al., 2003; Mease et al., 2011; Merrill et al., 2010; Orban et al., 2011; Rosenblum et al., 2012; Viglietta et al., 2008). While promising and currently used to treat several disorders, CTLA4-Ig lacked efficacy in moderate-to-severe human IBD (Sandborn et al., 2012). Indeed, RORγt$^+$ Treg cells are reduced in the intestine of patients with food allergy or IBD (Abdel-Gadir et al., 2019; Hepworth et al., 2015; Lyu et al., 2022), suggesting that CTLA4-Ig should be effective. However, RORγt$^+$ APCs expressing MHCII (signal one) are also numerically and functionally compromised in the inflamed gut environment of human IBD patients (Hepworth et al., 2015; Lyu et al., 2022). Given the key role of RORγt$^+$ APCs in instructing RORγt$^+$ Treg cells through signal one (Akagbosu et al., 2022; Kedmi et al., 2022; Lyu et al., 2022), we next sought to determine whether this CTLA4-Ig–mediated expansion of RORγt$^+$ Treg cells requires interplay with this pathway. To address this, we utilized

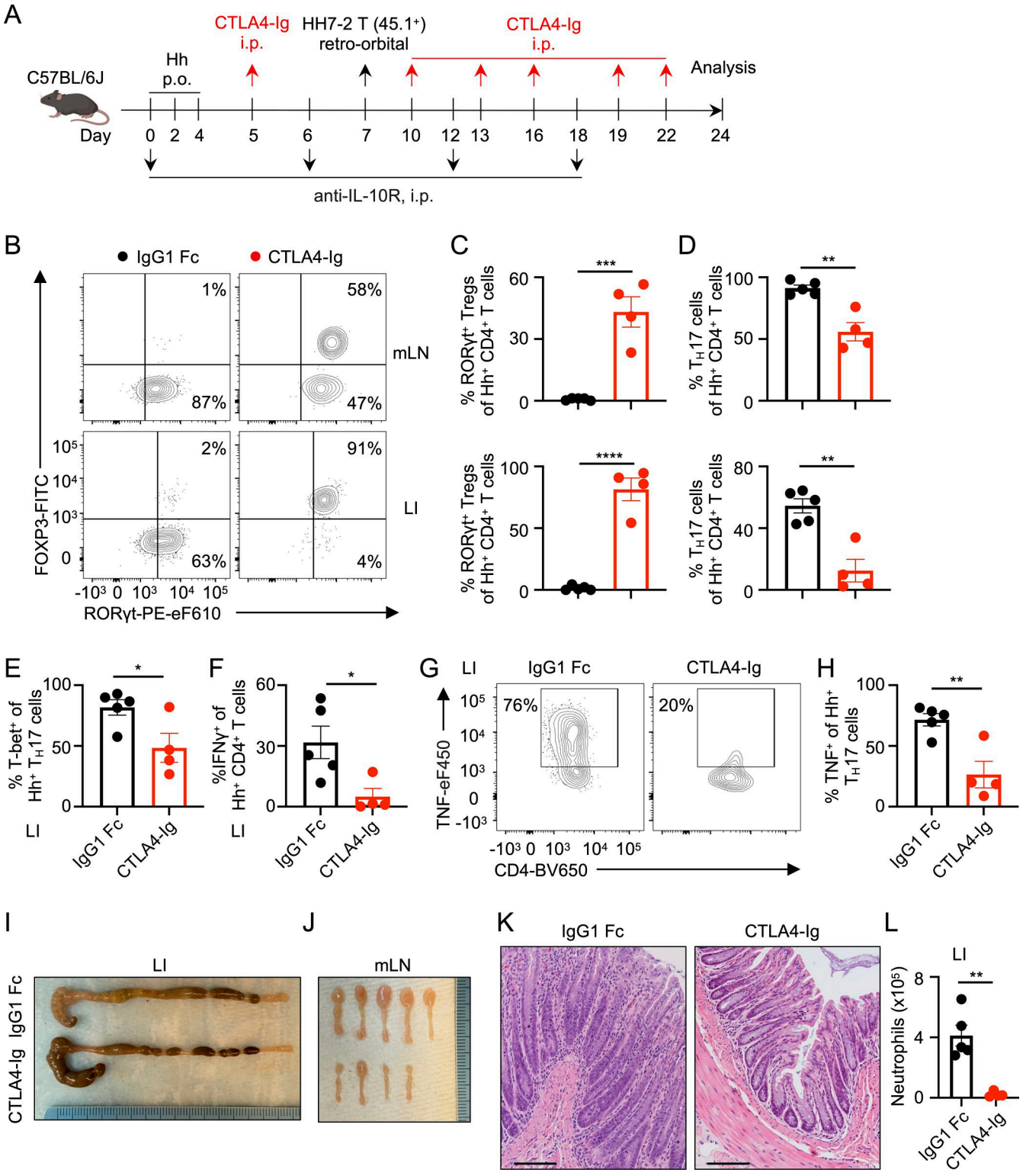

Figure 3. **CTLA4-Ig enforces microbiota-specific RORγt⁺ Treg cells and protects from gut inflammation. (A)** C57BL/6J WT mice were colonized with Hh on days 0, 2, and 4, followed by Hh-specific naïve CD4⁺ T cell transfer retro-orbitally on day 7; mice were i.p. injected with anti-IL-10R on days 0, 6, 12, and 18, and were i.p. injected with CTLA4-Ig on days 5, 10, 13, 16, 19, and 22. Mice were euthanized for analysis on day 24. **(B–D)** (B) Flow cytometry plots of the Hh-specific CD4⁺ T cells (mLN, top panel; LI, bottom panel) and frequencies of (C) Hh-specific RORγt⁺ Treg cells and (D) Hh-specific T_H17 cells in the mLN (top panel) and LI (bottom panel) of Hh-colonized WT mice treated with IgG1 Fc (n = 5) or CTLA4-Ig (n = 4). T_H17 cells were gated as CD4⁺ Foxp3⁻ RORγt⁺ T cells, and this strategy was applied consistently in all experiments. **(E and F)** Frequencies of (E) T-bet⁺ Hh-specific T_H17 cells and (F) IFNγ⁺ Hh-specific CD4⁺ T cells in LI of the WT mice in B. **(G and H)** (G) Flow cytometry plots and (H) frequency of TNF⁺ Hh-specific T_H17 cells in LI of the WT mice in B. **(I–K)** Images of (I) LI showing typhlocolitis, (J) enlarged mLNs, and (K) H&E staining of the distal colon in the WT mice in B. Scale bars, 100 µm. **(L)** Cell number of neutrophil infiltration in LI of the WT mice in B. The data in Fig. 3 are representative of two independent experiments. The data are shown as means ± SEM; the statistics shown in C, D, E, F, H, and L were obtained by unpaired Student's t test (two-tailed). *P < 0.05; **P < 0.01; ***P < 0.001; ****P < 0.0001.

RORγt^{Cre} *H2-Ab1*$^{fl/fl}$ mice with a selective deletion of MHCII on RORγt^{+} APCs (Hepworth et al., 2013; Hepworth et al., 2015), and found that in contrast to a blockade in IL-10R signaling, CTLA4-Ig was unable to overcome a defect in the generation of RORγt^{+} Treg cells in these mice (Fig. 4, A–C; and Fig. S1 E). Furthermore, we employed the mouse colitis model induced following Hh colonization combined with anti-IL-10R in RORγt^{Cre} *H2-Ab1*$^{fl/fl}$ mice versus littermate controls (Fig. S3 N). Strikingly, CTLA4-Ig treatment failed to restore Hh-specific RORγt^{+} Treg cells in both the mLN and LI of RORγt^{Cre} *H2-Ab1*$^{fl/fl}$ mice relative to that observed in littermate controls (Fig. 4, D–F). Rather, in this context and in contrast to littermate controls, mice lacking MHCII on RORγt^{+} APCs exhibited a significant increase in Hh-specific T_H17 cells and in their TNF production (Fig. 4, G–I). Importantly, CTLA4-Ig administration failed to ameliorate intestinal inflammation in RORγt^{Cre} *H2-Ab1*$^{fl/fl}$ mice, as evidenced by colon shortening, mLN enlargement, and significant neutrophil infiltration in the LI (Fig. 4, J–L). These findings demonstrate that MHCII-dependent signal one from RORγt^{+} APCs is required to enforce RORγt^{+} Treg cell generation when blocking costimulatory B7 signal two, and for associated protection from intestinal inflammation.

In summary, our collective findings identify that RORγt^{+} Treg cell generation undergoes a unique pathway independent of B7 costimulation, and rather, these signals antagonize this developmental program. This strikingly contrasts prior paradigms for conventional and thymic-derived Treg cells, which require B7-dependent costimulation for development, homeostasis, and function (Salomon et al., 2000; Tang et al., 2003). At the signaling level, CD28 ligation initiates multiple intracellular pathways that regulate T cell activation and differentiation. In addition to the well-characterized PI3K-Akt-Foxo1 axis (Brunet et al., 1999; Burke et al., 2024; Fabre et al., 2005; Ouyang et al., 2009; Shrestha et al., 2015), CD28 engagement activates NF-κB, MAPK, and mTOR signaling, which together control effector T cell survival, cytokine production, and metabolic reprogramming (Acuto and Michel, 2003; Chi, 2012; Esensten et al., 2016; Zhang et al., 1999). These pathways are also likely to influence RORγt^{+} Treg cell biology, given their close developmental and functional relationship to effector T_H17 cells, but how these signaling modules are mechanistically integrated in RORγt^{+} Treg cells remains incompletely understood and warrants further investigation. Separately, c-Maf is induced downstream of TCR, costimulatory, and cytokine signals and is essential for the development and suppressive function of RORγt^{+} Treg cells (Wheaton et al., 2017; Xu et al., 2018). How c-Maf is regulated downstream of B7-CD28 engagement in RORγt^{+} Treg cells, and how it in turn contributes to their differentiation and suppressive function, remains an important question for future studies.

Our findings also reveal that it is possible to harness existing therapeutics, such as gain-of-function or loss-of-function approaches with CTLA-4, to impact B7-dependent regulation of RORγt^{+} Treg cells in the gut. This may explain why intestinal inflammation is a frequent adverse event associated with CTLA-4 immune checkpoint blockade in cancer therapy (Bamias et al., 2017; Braun et al., 2025; Lo et al., 2024; Marthey et al., 2016). Further, our data demonstrate that CTLA4-Ig can be harnessed to enforce antigen-specific RORγt^{+} Treg cell responses and provide protection from experimental intestinal inflammation, which complements a recent study showing the therapeutic potential of this compound for enhancing oral tolerance to dietary antigens (Arai et al., 2026). In both contexts, the relevant cellular sources of costimulation that antagonizes immune tolerance remain unclear, where our new data reveal that it is not solely driven by B7 on either cDCs or RORγt^{+} APCs. Thus, it is likely dependent on multiple redundant sources, or on a unique source that has not yet been extensively explored, such as macrophages. Moreover, CTLA4-Ig likely acts through dual, complementary mechanisms to restore immune tolerance in the gut. On the one hand, CTLA4-Ig blocks B7-CD28 costimulation, limiting effector T cell activation and cytokine production (Tivol et al., 1995; Walunas et al., 1994; Walunas et al., 1996). On the other hand, our new data demonstrate that CTLA4-Ig increases the abundance of RORγt^{+} Treg cells, a cell type specialized in enforcing tolerance to gut microbiota and dietary antigens (Ohnmacht et al., 2015; Sefik et al., 2015). These observations align with prior findings that CTLA-4 regulates both effector and Treg cell compartments (Peggs et al., 2009), indicating that CTLA4-Ig promotes intestinal immune homeostasis by both restraining effector responses and enhancing RORγt^{+} Treg cell–mediated tolerance.

Intriguingly, in both our new data on intestinal inflammation, and in the recent study on oral tolerance to dietary antigens (Arai et al., 2026), CTLA4-Ig is effective only when signal one is simultaneously provided from either antigen presentation by RORγt^{+} APCs or continuous antigen feeding. This indicates that the key to driving optimal antigen-specific RORγt^{+} Treg cell responses and immune tolerance in the gut is to preserve a necessary MHCII-dependent signal one from RORγt^{+} APCs in the context of B7 costimulation blockade. Importantly, this provides one mechanistic explanation for the limited efficacy of CTLA4-Ig in clinical trials of human IBD with moderate-to-severe disease (Mayer et al., 2012; Sandborn et al., 2012). We propose that in the chronically inflamed human intestine, there is a previously reported dysregulation of RORγt^{+} APCs (Hepworth et al., 2015; Lyu et al., 2022), which restricts the availability of signal one and thereby uncouples costimulatory blockade from immune tolerance. In this setting, blockade of B7-CD28 interactions alone is insufficient to drive the expansion of antigen-specific RORγt^{+} Treg cells, despite effectively limiting effector T cell activation. Our data demonstrate that blockade of the B7 family of costimulatory molecules must act in concert with MHCII on RORγt^{+} APCs to promote RORγt^{+} Treg cell responses, providing a framework for understanding why CTLA4-Ig fails once gut inflammation is established. We previously showed that RORγt^{+} APCs can be therapeutically harnessed to drive antigen-specific Treg cells and enforce immune tolerance (Grigg et al., 2021). Thus, there is great promise that when combined with strategies to boost RORγt^{+} APCs, then B7 costimulatory signaling blockade with CTLA4-Ig or other approaches will be highly effective at driving antigen-specific RORγt^{+} Treg cell response and enforcing immune tolerance in the intestine.

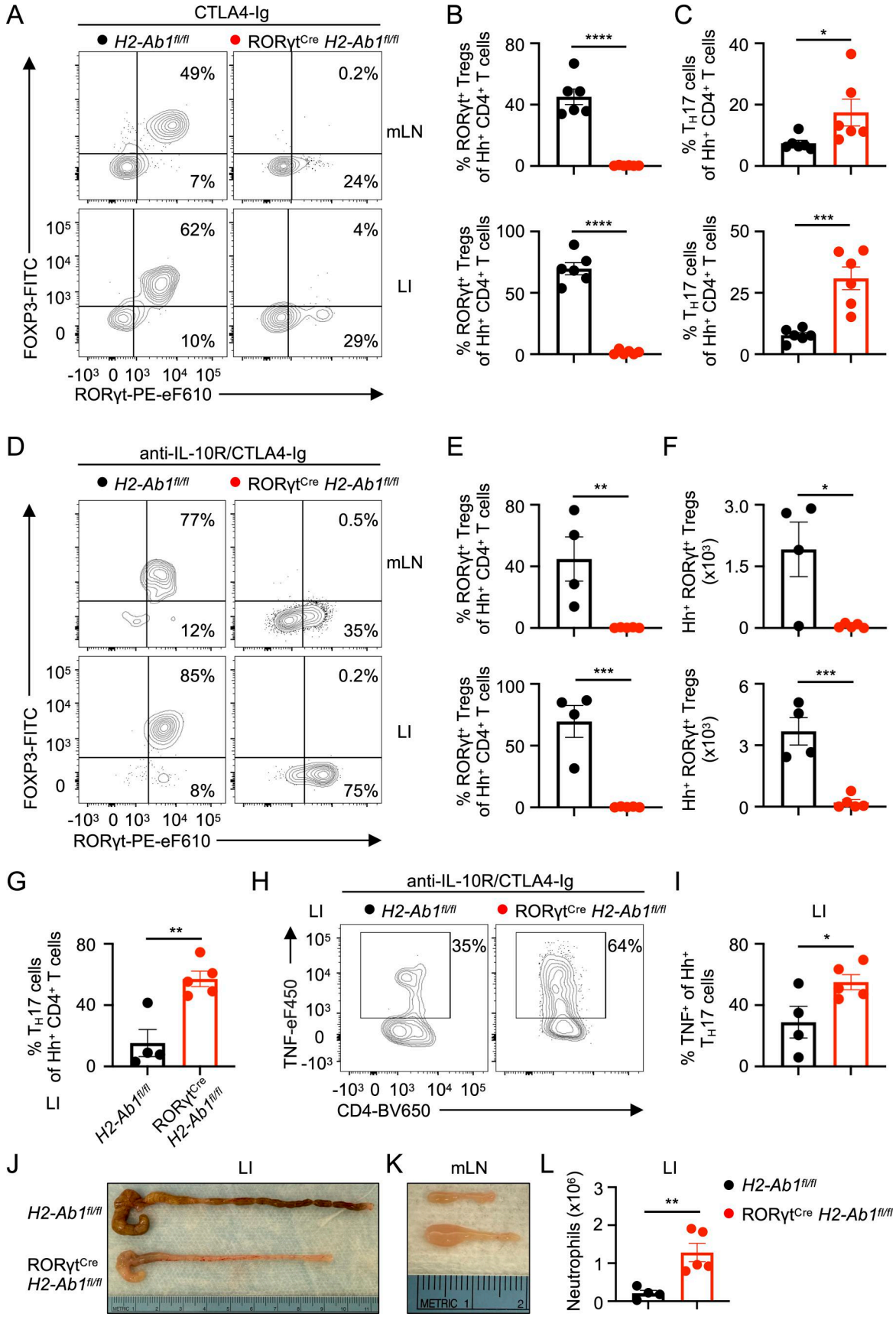

Figure 4. **RORγt⁺ APCs are required for CTLA4-Ig–driven immune tolerance. (A–C)** (A) Flow cytometry plots of the Hh-specific CD4⁺ T cells (mLN, top panel; LI, bottom panel) and frequencies of (B) Hh-specific RORγt⁺ Treg cells and (C) Hh-specific T_H17 cells in the mLN (top panel) and LI (bottom panel) of

H2-Ab1$^{fl/fl}$ mice (n = 6) and RORγt^{Cre} *H2-Ab1*$^{fl/fl}$ mice (n = 6). **(D–F)** (D) Flow cytometry plots of the Hh-specific CD4$^+$ T cells (mLN, top panel; LI, bottom panel), (E) frequency, and (F) cell number of Hh-specific RORγt$^+$ Treg cells in the mLN (top panel) and LI (bottom panel) of *H2-Ab1*$^{fl/fl}$ mice (n = 4) and RORγt^{Cre} *H2-Ab1*$^{fl/fl}$ mice (n = 5). **(G)** Frequency of Hh-specific T_H17 cells in LI of the mice in D. **(H and I)** (H) Flow cytometry plots and (I) frequency of TNF$^+$ Hh-specific T_H17 cells in LI of the mice in D. **(J–L)** Images of (J) LI showing typhlocolitis, (K) enlarged mLNs, and (L) cell number of neutrophil infiltration in the LI of the mice in D. The data in A–C are pooled from two independent experiments. The data in D–L are representative of two independent experiments. The data are shown as means ± SEM; the statistics shown in B, C, E, F, G, I, and L were obtained by unpaired Student's t test (two-tailed). *P < 0.05; **P < 0.01; ***P < 0.001; ****P < 0.0001.

Materials and methods

Mice

C57BL/6J mice, CD45.1 transgenic mice, *Cd80*$^{-/-}$/*Cd86*$^{-/-}$ mice (Borriello et al., 1997), CD80 Tg$^{fl/fl}$ mice (Watanabe et al., 2017), *H2-Ab1*$^{fl/fl}$ mice (Hashimoto et al., 2002), Hh (HH7-2) TCR transgenic mice (Xu et al., 2018), and *Clec9a*^{Cre} mice (Schraml et al., 2013) were purchased from Jackson Laboratories. RORγt^{Cre} mice (Lochner et al., 2008) were provided by Gérard Eberl (Institut Pasteur, Paris, France). All mice were on a C57BL/6 background and maintained in specific-pathogen-free facilities in Weill Cornell Medicine. Male and female mice were used at 5–12 wk of age. All protocols were approved by the Institutional Animal Care and Use Committee at Weill Cornell Medicine, and all experiments were performed in accordance with its guidelines.

Flow cytometry and cell sorting

Single-cell suspensions were incubated on ice with conjugated antibodies in PBS containing 2% FBS and 1 mM EDTA. Unlabeled anti-CD16/32 (clone 2.4G2, BD Biosciences) was used to block Fc receptors when analyzing myeloid cells. Dead cells were excluded with Fixable Aqua Dead Cell Stain (Thermo Fisher Scientific). The staining antibodies for flow cytometry were mainly purchased from Thermo Fisher Scientific, BioLegend, or BD Biosciences. The following were used for mouse cell-surface staining: CD3ε (145-2C11), CD4 (RM4-5, GK1.5), CD8a (53-6.7), CD5 (53-7.3), CD11b (M1/70), CD11c (N418), CD19 (1D3), CD64 (X54-5/7.1), GR1 (RB6-8C5), LY6G (1A8), CD45R (also known as B220; RA3-6B2), CD45.1 (A20), CD45.2 (104), CD45 (30-F11), CD90.2 (30-H12), CD127 (A7R34), MHCII (M5/114.15.2), NK1.1 (PK136), TCRγδ (GL3), CD44 (IM7), CD62L (MEL-14), CD25 (PC61), CXCR6 (SA051D1), NKR-P1B (also known as KLRB1B; 2D12), and TCR Vβ6 (RR4-7). The following were used for mouse intracellular staining: FOXP3 (FJK-16S), RORγt (B2D), PU.1 (also known as SPI1; 7C2C34), T-bet (4B10), IL-17A (17B7), IFNγ (XMG1.2), c-MAF (sym0F1), and TNFα (MP6-XT22). Lineage markers for mouse were as follows: CD3ε, CD5, CD19, B220, GR1, NK1.1, and TCRγδ, unless otherwise indicated.

For intracellular staining, cells were fixed and permeabilized with FoxP3/Transcription Factor Staining Buffer Set following the manufacturer's instructions (Thermo Fisher Scientific). Briefly, cells were incubated with FoxP3 Fixation/Permeabilization working solution for 30 min at room temperature or overnight at 4°C and then stained for intracellular targets by incubating with conjugated antibodies in 1× permeabilization buffer for 45 min at room temperature. For intracellular cytokine staining, cells were first incubated for 4 h in RPMI with 10% FBS, 50 ng/ml phorbol 12-myristate 13-acetate, 750 ng/ml ionomycin, and 10 µg/ml brefeldin A, all obtained from Sigma-Aldrich. Antibodies for flow cytometry were purchased from BioLegend, Thermo Fisher Scientific, or BD Biosciences. Flow cytometry data were collected using an LSRFortessa (BD Biosciences) and analyzed with FlowJo V10 software (Tree Star). Cell sorting was performed with an Aria II (BD Biosciences).

Preparation of single-cell suspensions from intestine or lymph nodes

LI including cecum and colon was removed, opened longitudinally, and rinsed with ice-cold PBS. Dissected intestinal tissues were cut into pieces of ∼0.5 cm, and intestinal epithelial cells were dissociated by incubating in HBSS (Sigma-Aldrich) containing 5 mM EDTA (Thermo Fisher Scientific), 1 mM dithiothreitol (Sigma-Aldrich), and 2% FBS with shaking at 200 rpm for 20 min at 37°C. Dissociation of epithelial cells was performed twice. Samples were vortexed and rinsed with PBS after each step. The epithelial cell fraction was discarded. Remaining tissues were minced and enzymatically digested in RPMI containing 0.4 U/ml dispase (Thermo Fisher Scientific), 1 mg/ml collagenase III (Worthington), 20 µg/ml DNase I (Sigma-Aldrich), and 10% FBS on a shaker for 45 min at 37°C. Leukocytes were enriched by 40% (for flow cytometry) or 40/80% (for sorting) Percoll (GE Healthcare) gradient centrifugation. mLNs were chopped and incubated in RPMI containing 2% FBS and 1 mg/ml collagenase II (Sigma-Aldrich), 20 µg/ml DNase I (Sigma-Aldrich) with shaking at 200 rpm for 20 min at 37°C, and cells were then dissociated using a Pasteur pipette, and filtered through a 70-µm cell strainer in PBS containing 0.5 mM EDTA and 2% FBS.

CTLA4-Ig binding assay

Following preparation of single-cell suspensions from the LI and mLN, 10^6 cells per condition were seeded into individual wells of a 96-well plate and incubated with CTLA4-Ig (100 µg/ml) at 4°C for 30 min. Cells were then washed twice with PBS to remove unbound reagent and immediately processed for flow cytometry staining. To detect cell-bound CTLA4-Ig, cells were stained with a PE-conjugated AffiniPure F(ab′)$_2$ fragment donkey anti-human IgG antibody (Jackson ImmunoResearch Laboratories), and the presence of CTLA4-Ig was quantified by flow cytometry. To control for nonspecific Fc-mediated binding, parallel samples were incubated with total human IgG and processed identically. PBS-treated cells were included as a negative control.

Hh-specific TCR transgenic T cells and Hh-induced colitis model

Recipient mice (CD45.2$^+$) were colonized with Hh (ATCC 51449/Hh3B1) by oral gavage (p.o.) with 3 doses every other day within 7 days before T cell transfer, using a protocol adapted from

previously described methods (Lyu et al., 2022; Xu et al., 2018). Naïve CD4$^+$ T cells of Hh (HH7-2) TCR transgenic mice (CD45.1$^+$) were isolated from spleen and lymph nodes by a FACSAria cell sorter (BD Biosciences) and were gated as CD45.1$^+$CD5$^+$CD4$^+$CD25$^-$CD44^{low}CD62L^{hi}TCR Vβ6$^+$. Recipient mice received 100,000 cells per mouse of HH7-2 TCR transgenic naïve CD4$^+$ T cells retro-orbitally and were analyzed 2 wk after transfer, unless otherwise indicated. To induce colitis, mice were orally gavaged with Hh (ATCC 51449/Hh3B1), followed by intraperitoneal (i.p.) administration of anti-IL-10R antibody (clone 1B1.3A, BioXcell; 800 µg/mouse) on day 0 and every 6 days thereafter. Where indicated, mice were administered an i.p. injection of anti-CD80 (clone 16-10A1, BioXcell; 1 mg/mouse) and anti-CD86 (clone GL-1, BioXcell; 1 mg/mouse), with IgG2a/2b isotype antibodies (clone 2A3/clone LTF-2, BioXcell; 1 mg/mouse) as controls. In separate experiments, CTLA4-Ig fusion protein (clone CTLA-4-Ig (hum/hum), BioXcell; 200 µg/mouse) or anti-CTLA4 (clone 9D9, BioXcell; 200 µg/mouse) was administered i.p., with IgG1 Fc (clone human Fc-G1, BioXcell; 200 µg/mouse) or IgG2b (clone MPC-11, BioXcell; 200 µg/mouse) serving as the respective controls.

Histology

Distal LI tissues were fixed in 4% paraformaldehyde and embedded in paraffin. 5-µm sections were stained with H&E. Images were taken using a Nikon Eclipse Ti microscope and NIS-Elements 4.30.02 software (Nikon).

Statistics

P values for datasets were determined by unpaired two-tailed Student's *t* test or ordinary one-way ANOVA with 95% confidence intervals. All statistical analyses were performed with GraphPad Prism version 10 (GraphPad Software Inc.). *P* values <0.05 were considered significant.

Online supplemental material

Fig. S1 shows the experimental designs for B7 costimulation blockade and CTLA4-Ig or anti-CTLA4 administration in a mouse model with Hh colonization and the development of Hh-specific RORγt$^+$ Treg cells in the mLN and LI. It also presents Hh-specific and endogenous T cell changes in the mLN and LI of these mice. Fig. S2 illustrates the flow cytometry gating strategy developed in this study to identify major APC subsets and to quantify CTLA4-Ig binding across populations. It also demonstrates the CTLA4-Ig–induced changes in the frequency and absolute number of multiple APC subsets in the mLN and LI of C57BL/6J WT mice. Fig. S3 demonstrates the immune profiling in the Hh-induced colitis model, including c-Maf expression in Hh-specific RORγt$^+$ T cells and phenotypic and inflammatory cytokine changes in endogenous RORγt$^+$ T cells following IgG1 Fc or CTLA4-Ig treatment. It also shows the experimental designs for colitis induction by Hh colonization plus anti-IL-10R blockade, and for CTLA4-Ig treatment in RORγt^{Cre} *H2-Ab1*$^{fl/fl}$ mice and associated littermate controls.

Data availability

All data in the article and its supplementary materials are available upon request from the corresponding authors. The sequencing data used to generate Fig. S2 A are publicly available from the Gene Expression Omnibus under the accession number GSE184175.

Acknowledgments

We acknowledge members of the Sonnenberg Laboratory for discussions and critical reading of the manuscript. The illustrations in this manuscript were created in BioRender (https://BioRender.com).

Research in the Sonnenberg Laboratory is supported by the National Institutes of Health (R01AI143842, R01AI123368, R01AI145989, U01AI095608, R01AI162936, R37AI174468, and R01CA274534), an Investigators in the Pathogenesis of Infectious Disease Award from the Burroughs Wellcome Fund, the Meyer Cancer Center Collaborative Research Initiative, the Dalton Family Foundation, and Linda and Glenn Greenberg. G.F. Sonnenberg is a CRI Lloyd J. Old STAR. M. Lyu is supported by the National Institutes of Health (K99CA290052).

Author contributions: Mengze Lyu: conceptualization, data curation, formal analysis, funding acquisition, investigation, methodology, project administration, resources, software, supervision, validation, visualization, and writing—original draft, review, and editing. Gregory F. Sonnenberg: conceptualization, data curation, formal analysis, funding acquisition, investigation, methodology, project administration, resources, software, supervision, validation, visualization, and writing—original draft, review, and editing.

Disclosures: The authors declare no competing interests exist.

Submitted: 28 May 2025
Revised: 5 February 2026
Accepted: 20 March 2026

References

Abdel-Gadir, A., E. Stephen-Victor, G.K. Gerber, M. Noval Rivas, S. Wang, H. Harb, L. Wang, N. Li, E. Crestani, S. Spielman, et al. 2019. Microbiota therapy acts via a regulatory T cell MyD88/RORgammat pathway to suppress food allergy. *Nat. Med.* 25:1164–1174. https://doi.org/10.1038/s41591-019-0461-z

Acuto, O., and F. Michel. 2003. CD28-mediated co-stimulation: A quantitative support for TCR signalling. *Nat. Rev. Immunol.* 3:939–951. https://doi.org/10.1038/nri1248

Akagbosu, B., Z. Tayyebi, G. Shibu, Y.A. Paucar Iza, D. Deep, Y.F. Parisotto, L. Fisher, H.A. Pasolli, V. Thevin, R. Elmentaite, et al. 2022. Novel antigen-presenting cell imparts T(reg)-dependent tolerance to gut microbiota. *Nature*. 610:752–760. https://doi.org/10.1038/s41586-022-05309-5

Al Nabhani, Z., S. Dulauroy, R. Marques, C. Cousu, S. Al Bounny, F. Dejardin, T. Sparwasser, M. Berard, N. Cerf-Bensussan, and G. Eberl. 2019. A weaning reaction to microbiota is required for resistance to immunopathologies in the adult. *Immunity*. 50:1276–1288.e5. https://doi.org/10.1016/j.immuni.2019.02.014

Appleman, L.J., A.A. van Puijenbroek, K.M. Shu, L.M. Nadler, and V.A. Boussiotis. 2002. CD28 costimulation mediates down-regulation of p27kip1 and cell cycle progression by activation of the PI3K/PKB signaling pathway in primary human T cells. *J. Immunol.* 168:2729–2736. https://doi.org/10.4049/jimmunol.168.6.2729

Arai, M., R. Kawakami, Y. Nakamura, Y. Naito, D. Motooka, A. Sugimoto, T. Kimoto, N. Ohkura, N. Mikami, and S. Sakaguchi. 2026. Oral antigen exposure under costimulation blockade induces Treg cells to establish

immune tolerance. *J. Exp. Med.* 223:e20251635. https://doi.org/10.1084/jem.20251635

Azuma, M., D. Ito, H. Yagita, K. Okumura, J.H. Phillips, L.L. Lanier, and C. Somoza. 1993. B70 antigen is a second ligand for CTLA-4 and CD28. *Nature*. 366:76–79. https://doi.org/10.1038/366076a0

Bamias, G., I. Delladetsima, M. Perdiki, S.I. Siakavellas, D. Goukos, G.V. Papatheodoridis, G.L. Daikos, and H. Gogas. 2017. Immunological characteristics of colitis associated with anti-CTLA-4 antibody therapy. *Cancer Invest.* 35:443–455. https://doi.org/10.1080/07357907.2017.1324032

Barata, J.T., A. Silva, J.G. Brandao, L.M. Nadler, A.A. Cardoso, and V.A. Boussiotis. 2004. Activation of PI3K is indispensable for interleukin 7-mediated viability, proliferation, glucose use, and growth of T cell acute lymphoblastic leukemia cells. *J. Exp. Med.* 200:659–669. https://doi.org/10.1084/jem.20040789

Borriello, F., M.P. Sethna, S.D. Boyd, A.N. Schweitzer, E.A. Tivol, D. Jacoby, T.B. Strom, E.M. Simpson, G.J. Freeman, and A.H. Sharpe. 1997. B7-1 and B7-2 have overlapping, critical roles in immunoglobulin class switching and germinal center formation. *Immunity*. 6:303–313. https://doi.org/10.1016/s1074-7613(00)80333-7

Braun, L.M., Y. Lu, and R. Zeiser. 2025. Clinical perspective and treatment of immune-related colitis after cancer immunotherapy. *Trends Cancer*. 11:1058–1077. https://doi.org/10.1016/j.trecan.2025.07.005

Brunet, A., A. Bonni, M.J. Zigmond, M.Z. Lin, P. Juo, L.S. Hu, M.J. Anderson, K.C. Arden, J. Blenis, and M.E. Greenberg. 1999. Akt promotes cell survival by phosphorylating and inhibiting a Forkhead transcription factor. *Cell*. 96:857–868. https://doi.org/10.1016/s0092-8674(00)80595-4

Burke, K.P., A. Chaudhri, G.J. Freeman, and A.H. Sharpe. 2024. The B7:CD28 family and friends: Unraveling coinhibitory interactions. *Immunity*. 57:223–244. https://doi.org/10.1016/j.immuni.2024.01.013

Cabric, V., Y. Franco Parisotto, T. Park, B. Akagbosu, Z. Zhao, Y. Lo, G. Shibu, L. Fisher, Y.A. Paucar Iza, C. Leslie, and C.C. Brown. 2025. A wave of thetis cells imparts tolerance to food antigens early in life. *Science*. 389:268–274. https://doi.org/10.1126/science.adp0535

Caux, C., B. Vanbervliet, C. Massacrier, M. Azuma, K. Okumura, L.L. Lanier, and J. Banchereau. 1994. B70/B7-2 is identical to CD86 and is the major functional ligand for CD28 expressed on human dendritic cells. *J. Exp. Med.* 180:1841–1847. https://doi.org/10.1084/jem.180.5.1841

Chi, H. 2012. Regulation and function of mTOR signalling in T cell fate decisions. *Nat. Rev. Immunol.* 12:325–338. https://doi.org/10.1038/nri3198

Collins, A.V., D.W. Brodie, R.J. Gilbert, A. Iaboni, R. Manso-Sancho, B. Walse, D.I. Stuart, P.A. van der Merwe, and S.J. Davis. 2002. The interaction properties of costimulatory molecules revisited. *Immunity*. 17:201–210. https://doi.org/10.1016/s1074-7613(02)00362-x

Davenport, C.M., H.A. McAdams, J. Kou, K. Mascioli, C. Eichman, L. Healy, J. Peterson, S. Murphy, D. Coppola, and A. Truneh. 2002. Inhibition of pro-inflammatory cytokine generation by CTLA4-Ig in the skin and colon of mice adoptively transplanted with CD45RBhi CD4+ T cells correlates with suppression of psoriasis and colitis. *Int. Immunopharmacol.* 2:653–672. https://doi.org/10.1016/s1567-5769(01)00201-6

Dobes, J., O. Ben-Nun, A. Binyamin, L. Stoler-Barak, B.E. Oftedal, Y. Goldfarb, N. Kadouri, Y. Gruper, T. Givony, I. Zalayat, et al. 2022. Extrathymic expression of Aire controls the induction of effective T(H)17 cell-mediated immune response to Candida albicans. *Nat. Immunol.* 23:1098–1108. https://doi.org/10.1038/s41590-022-01247-6

Esensten, J.H., Y.A. Helou, G. Chopra, A. Weiss, and J.A. Bluestone. 2016. CD28 costimulation: From mechanism to therapy. *Immunity*. 44:973–988. https://doi.org/10.1016/j.immuni.2016.04.020

Fabre, S., V. Lang, J. Harriague, A. Jobart, T.G. Unterman, A. Trautmann, and G. Bismuth. 2005. Stable activation of phosphatidylinositol 3-kinase in the T cell immunological synapse stimulates Akt signaling to FoxO1 nuclear exclusion and cell growth control. *J. Immunol.* 174:4161–4171. https://doi.org/10.4049/jimmunol.174.7.4161

Freeman, G.J., J.G. Gribben, V.A. Boussiotis, J.W. Ng, V.A. Restivo Jr, L.A. Lombard, G.S. Gray, and L.M. Nadler. 1993. Cloning of B7-2: A CTLA-4 counter-receptor that costimulates human T cell proliferation. *Science*. 262:909–911. https://doi.org/10.1126/science.7694363

Fu, L., R. Upadhyay, M. Pokrovskii, F.M. Chen, G. Romero-Meza, A. Griesemer, and D.R. Littman. 2025. Prdm16-dependent antigen-presenting cells induce tolerance to gut antigens. *Nature*. 642:756–765. https://doi.org/10.1038/s41586-025-08982-4

Glocker, E.O., D. Kotlarz, K. Boztug, E.M. Gertz, A.A. Schaffer, F. Noyan, M. Perro, J. Diestelhorst, A. Allroth, D. Murugan, et al. 2009. Inflammatory bowel disease and mutations affecting the interleukin-10 receptor. *N. Engl. J. Med.* 361:2033–2045. https://doi.org/10.1056/NEJMoa0907206

Goc, J., M. Lv, N.J. Bessman, A.L. Flamar, S. Sahota, H. Suzuki, F. Teng, G.G. Putzel, JRI Live Cell Bank, G. Eberl, et al. 2021. Dysregulation of ILC3s unleashes progression and immunotherapy resistance in colon cancer. *Cell*. 184:5015–5030.e16. https://doi.org/10.1016/j.cell.2021.07.029

Green, J.M., P.J. Noel, A.I. Sperling, T.L. Walunas, G.S. Gray, J.A. Bluestone, and C.B. Thompson. 1994. Absence of B7-dependent responses in CD28-deficient mice. *Immunity*. 1:501–508. https://doi.org/10.1016/1074-7613(94)90092-2

Grigg, J.B., A. Shanmugavadivu, T. Regen, C.N. Parkhurst, A. Ahmed, A.M. Joseph, M. Mazzucco, K. Gronke, A. Diefenbach, G. Eberl, et al. 2021. Antigen-presenting innate lymphoid cells orchestrate neuroinflammation. *Nature*. 600:707–712. https://doi.org/10.1038/s41586-021-04136-4

Hashimoto, K., S.K. Joshi, and P.A. Koni. 2002. A conditional null allele of the major histocompatibility IA-beta chain gene. *Genesis*. 32:152–153. https://doi.org/10.1002/gene.10056

Hepworth, M.R., T.C. Fung, S.H. Masur, J.R. Kelsen, F.M. McConnell, J. Dubrot, D.R. Withers, S. Hugues, M.A. Farrar, W. Reith, et al. 2015. Immune tolerance. Group 3 innate lymphoid cells mediate intestinal selection of commensal bacteria-specific CD4(+) T cells. *Science*. 348:1031–1035. https://doi.org/10.1126/science.aaa4812

Hepworth, M.R., L.A. Monticelli, T.C. Fung, C.G. Ziegler, S. Grunberg, R. Sinha, A.R. Mantegazza, H.L. Ma, A. Crawford, J.M. Angelosanto, et al. 2013. Innate lymphoid cells regulate CD4+ T-cell responses to intestinal commensal bacteria. *Nature*. 498:113–117. https://doi.org/10.1038/nature12240

Kedmi, R., T.A. Najar, K.R. Mesa, A. Grayson, L. Kroehling, Y. Hao, S. Hao, M. Pokrovskii, M. Xu, J. Talbot, et al. 2022. A RORgammat(+) cell instructs gut microbiota-specific T(reg) cell differentiation. *Nature*. 610:737–743. https://doi.org/10.1038/s41586-022-05089-y

Kelsen, J.R., R.N. Baldassano, D. Artis, and G.F. Sonnenberg. 2015. Maintaining intestinal health: The genetics and immunology of very early onset inflammatory bowel disease. *Cell Mol. Gastroenterol. Hepatol.* 1:462–476. https://doi.org/10.1016/j.jcmgh.2015.06.010

Kim, K.S., S.W. Hong, D. Han, J. Yi, J. Jung, B.G. Yang, J.Y. Lee, M. Lee, and C.D. Surh. 2016. Dietary antigens limit mucosal immunity by inducing regulatory T cells in the small intestine. *Science*. 351:858–863. https://doi.org/10.1126/science.aac5560

Knoop, K.A., K.G. McDonald, P.E. Coughlin, D.H. Kulkarni, J.K. Gustafsson, B. Rusconi, V. John, I.M. Ndao, A. Beigelman, M. Good, et al. 2020. Synchronization of mothers and offspring promotes tolerance and limits allergy. *JCI Insight*. 5:e137943. https://doi.org/10.1172/jci.insight.137943

Kremer, J.M., M. Dougados, P. Emery, P. Durez, J. Sibilia, W. Shergy, S. Steinfeld, E. Tindall, J.C. Becker, T. Li, et al. 2005. Treatment of rheumatoid arthritis with the selective costimulation modulator abatacept: Twelve-month results of a phase iib, double-blind, randomized, placebo-controlled trial. *Arthritis Rheum.* 52:2263–2271. https://doi.org/10.1002/art.21201

Kremer, J.M., H.K. Genant, L.W. Moreland, A.S. Russell, P. Emery, C. Abud-Mendoza, J. Szechinski, T. Li, Z. Ge, J.C. Becker, and R. Westhovens. 2006. Effects of abatacept in patients with methotrexate-resistant active rheumatoid arthritis: A randomized trial. *Ann. Intern. Med.* 144:865–876. https://doi.org/10.7326/0003-4819-144-12-200606200-00003

Kremer, J.M., R. Westhovens, M. Leon, E. Di Giorgio, R. Alten, S. Steinfeld, A. Russell, M. Dougados, P. Emery, I.F. Nuamah, et al. 2003. Treatment of rheumatoid arthritis by selective inhibition of T-cell activation with fusion protein CTLA4Ig. *N. Engl. J. Med.* 349:1907–1915. https://doi.org/10.1056/NEJMoa035075

Kullberg, M.C., D. Jankovic, C.G. Feng, S. Hue, P.L. Gorelick, B.S. McKenzie, D.J. Cua, F. Powrie, A.W. Cheever, K.J. Maloy, and A. Sher. 2006. IL-23 plays a key role in helicobacter hepaticus-induced T cell-dependent colitis. *J. Exp. Med.* 203:2485–2494. https://doi.org/10.1084/jem.20061082

Kullberg, M.C., A.G. Rothfuchs, D. Jankovic, P. Caspar, T.A. Wynn, P.L. Gorelick, A.W. Cheever, and A. Sher. 2001. Helicobacter hepaticus-induced colitis in interleukin-10-deficient mice: Cytokine requirements for the induction and maintenance of intestinal inflammation. *Infect. Immun.* 69:4232–4241. https://doi.org/10.1128/IAI.69.7.4232-4241.2001

Kullberg, M.C., J.M. Ward, P.L. Gorelick, P. Caspar, S. Hieny, A. Cheever, D. Jankovic, and A. Sher. 1998. Helicobacter hepaticus triggers colitis in specific-pathogen-free interleukin-10 (IL-10)-deficient mice through an IL-12- and gamma interferon-dependent mechanism. *Infect. Immun.* 66:5157–5166. https://doi.org/10.1128/IAI.66.11.5157-5166.1998

Leach, D.R., M.F. Krummel, and J.P. Allison. 1996. Enhancement of antitumor immunity by CTLA-4 blockade. *Science*. 271:1734–1736. https://doi.org/10.1126/science.271.5256.1734

Lenschow, D.J., T.L. Walunas, and J.A. Bluestone. 1996. CD28/B7 system of T cell costimulation. *Annu. Rev. Immunol.* 14:233–258. https://doi.org/10.1146/annurev.immunol.14.1.233

Linsley, P.S., W. Brady, M. Urnes, L.S. Grosmaire, N.K. Damle, and J.A. Ledbetter. 1991. CTLA-4 is a second receptor for the B cell activation antigen B7. *J. Exp. Med.* 174:561–569. https://doi.org/10.1084/jem.174.3.561

Linsley, P.S., and J.A. Ledbetter. 1993. The role of the CD28 receptor during T cell responses to antigen. *Annu. Rev. Immunol.* 11:191–212. https://doi.org/10.1146/annurev.iy.11.040193.001203

Lo, B.C., I. Kryczek, J. Yu, L. Vatan, R. Caruso, M. Matsumoto, Y. Sato, M.H. Shaw, N. Inohara, Y. Xie, et al. 2024. Microbiota-dependent activation of CD4(+) T cells induces CTLA-4 blockade-associated colitis via Fcgamma receptors. *Science*. 383:62–70. https://doi.org/10.1126/science.adh8342

Lochner, M., L. Peduto, M. Cherrier, S. Sawa, F. Langa, R. Varona, D. Riethmacher, M. Si-Tahar, J.P. Di Santo, and G. Eberl. 2008. In vivo equilibrium of proinflammatory IL-17+ and regulatory IL-10+ Foxp3+ RORgamma t+ T cells. *J. Exp. Med.* 205:1381–1393. https://doi.org/10.1084/jem.20080034

Lyu, M., H. Suzuki, L. Kang, F. Gaspal, W. Zhou, J. Goc, L. Zhou, J. Zhou, W. Zhang, J.R.I.L.C. Bank, et al. 2022. ILC3s select microbiota-specific regulatory T cells to establish tolerance in the gut. *Nature*. 610:744–751. https://doi.org/10.1038/s41586-022-05141-x

Marthey, L., C. Mateus, C. Mussini, M. Nachury, S. Nancey, F. Grange, C. Zallot, L. Peyrin-Biroulet, J.F. Rahier, M. Bourdier de Beauregard, et al. 2016. Cancer immunotherapy with anti-CTLA-4 monoclonal antibodies induces an inflammatory bowel disease. *J. Crohns Colitis*. 10:395–401. https://doi.org/10.1093/ecco-jcc/jjv227

Mayer, L., A. Kaser, and R.S. Blumberg. 2012. Dead on arrival: Understanding the failure of CTLA4-immunoglobulin therapy in inflammatory bowel disease. *Gastroenterology*. 143:13–17. https://doi.org/10.1053/j.gastro.2012.05.015

Mease, P., M.C. Genovese, G. Gladstein, A.J. Kivitz, C. Ritchlin, P.P. Tak, J. Wollenhaupt, O. Bahary, J.C. Becker, S. Kelly, et al. 2011. Abatacept in the treatment of patients with psoriatic arthritis: Results of a six-month, multicenter, randomized, double-blind, placebo-controlled, phase II trial. *Arthritis Rheum.* 63:939–948. https://doi.org/10.1002/art.30176

Merrill, J.T., R. Burgos-Vargas, R. Westhovens, A. Chalmers, D. D'Cruz, D.J. Wallace, S.C. Bae, L. Sigal, J.C. Becker, S. Kelly, et al. 2010. The efficacy and safety of abatacept in patients with non-life-threatening manifestations of systemic lupus erythematosus: Results of a twelve-month, multicenter, exploratory, phase IIb, randomized, double-blind, placebo-controlled trial. *Arthritis Rheum.* 62:3077–3087. https://doi.org/10.1002/art.27601

Moreland, L., G. Bate, and P. Kirkpatrick. 2006. Abatacept. *Nat. Rev. Drug Discov.* 5:185–186. https://doi.org/10.1038/nrd1989

Narasimhan, H., M.L. Richter, R. Shakiba, N.E. Papaioannou, C. Stehle, K. Ravi Rengarajan, I. Ulmert, A. Kendirli, C. de la Rosa, P.Y. Kuo, et al. 2025. RORgammat-expressing dendritic cells are functionally versatile and evolutionarily conserved antigen-presenting cells. *Proc. Natl. Acad. Sci. USA*. 122:e2417308122. https://doi.org/10.1073/pnas.2417308122

Ohnmacht, C., J.H. Park, S. Cording, J.B. Wing, K. Atarashi, Y. Obata, V. Gaboriau-Routhiau, R. Marques, S. Dulauroy, M. Fedoseeva, et al. 2015. MUCOSAL IMMUNOLOGY. The microbiota regulates type 2 immunity through RORgammat(+) T cells. *Science*. 349:989–993. https://doi.org/10.1126/science.aac4263

Orban, T., B. Bundy, D.J. Becker, L.A. DiMeglio, S.E. Gitelman, R. Goland, P.A. Gottlieb, C.J. Greenbaum, J.B. Marks, R. Monzavi, et al. 2011. Co-stimulation modulation with abatacept in patients with recent-onset type 1 diabetes: A randomised, double-blind, placebo-controlled trial. *Lancet*. 378:412–419. https://doi.org/10.1016/S0140-6736(11)60886-6

Ouyang, W., O. Beckett, R.A. Flavell, and M.O. Li. 2009. An essential role of the Forkhead-box transcription factor Foxo1 in control of T cell homeostasis and tolerance. *Immunity*. 30:358–371. https://doi.org/10.1016/j.immuni.2009.02.003

Peggs, K.S., S.A. Quezada, C.A. Chambers, A.J. Korman, and J.P. Allison. 2009. Blockade of CTLA-4 on both effector and regulatory T cell compartments contributes to the antitumor activity of anti-CTLA-4 antibodies. *J. Exp. Med.* 206:1717–1725. https://doi.org/10.1084/jem.20082492

Ramanan, D., E. Sefik, S. Galvan-Pena, M. Wu, L. Yang, Z. Yang, A. Kostic, T.V. Golovkina, D.L. Kasper, D. Mathis, and C. Benoist. 2020. An immunologic mode of multigenerational transmission governs a gut Treg setpoint. *Cell*. 181:1276–1290.e13. https://doi.org/10.1016/j.cell.2020.04.030

Read, S., V. Malmstrom, and F. Powrie. 2000. Cytotoxic T lymphocyte-associated antigen 4 plays an essential role in the function of CD25(+)CD4(+) regulatory cells that control intestinal inflammation. *J. Exp. Med.* 192:295–302. https://doi.org/10.1084/jem.192.2.295

Rodrigues, P.F., S. Wu, T. Trsan, S.K. Panda, J.L. Fachi, Y. Liu, S. Du, S. de Oliveira, A.U. Antonova, D. Khantakova, et al. 2025. Rorgammat-positive dendritic cells are required for the induction of peripheral regulatory T cells in response to oral antigens. *Cell*. 188:2720–2737.e22. https://doi.org/10.1016/j.cell.2025.03.020

Rosenblum, M.D., I.K. Gratz, J.S. Paw, and A.K. Abbas. 2012. Treating human autoimmunity: Current practice and future prospects. *Sci. Transl. Med.* 4:125sr121. https://doi.org/10.1126/scitranslmed.3003504

Ruperto, N., D.J. Lovell, P. Quartier, E. Paz, N. Rubio-Perez, C.A. Silva, C. Abud-Mendoza, R. Burgos-Vargas, V. Gerloni, J.A. Melo-Gomes, et al. 2008. Abatacept in children with juvenile idiopathic arthritis: A randomised, double-blind, placebo-controlled withdrawal trial. *Lancet*. 372:383–391. https://doi.org/10.1016/S0140-6736(08)60998-8

Salomon, B., D.J. Lenschow, L. Rhee, N. Ashourian, B. Singh, A. Sharpe, and J.A. Bluestone. 2000. B7/CD28 costimulation is essential for the homeostasis of the CD4+CD25+ immunoregulatory T cells that control autoimmune diabetes. *Immunity*. 12:431–440. https://doi.org/10.1016/s1074-7613(00)80195-8

Sandborn, W.J., J.F. Colombel, B.E. Sands, P. Rutgeerts, S.R. Targan, R. Panaccione, B. Bressler, K. Geboes, S. Schreiber, R. Aranda, et al. 2012. Abatacept for Crohn's disease and ulcerative colitis. *Gastroenterology*. 143:62–69.e4. https://doi.org/10.1053/j.gastro.2012.04.010

Schraml, B.U., J. van Blijswijk, S. Zelenay, P.G. Whitney, A. Filby, S.E. Acton, N.C. Rogers, N. Moncaut, J.J. Carvajal, and C. Reis e Sousa. 2013. Genetic tracing via DNGR-1 expression history defines dendritic cells as a hematopoietic lineage. *Cell*. 154:843–858. https://doi.org/10.1016/j.cell.2013.07.014

Schwartz, J.C., X. Zhang, A.A. Fedorov, S.G. Nathenson, and S.C. Almo. 2001. Structural basis for co-stimulation by the human CTLA-4/B7-2 complex. *Nature*. 410:604–608. https://doi.org/10.1038/35069112

Sefik, E., N. Geva-Zatorsky, S. Oh, L. Konnikova, D. Zemmour, A.M. McGuire, D. Burzyn, A. Ortiz-Lopez, M. Lobera, J. Yang, et al. 2015. MUCOSAL IMMUNOLOGY. Individual intestinal symbionts induce a distinct population of RORgamma(+) regulatory T cells. *Science*. 349:993–997. https://doi.org/10.1126/science.aaa9420

Sharpe, A.H., and G.J. Freeman. 2002. The B7-CD28 superfamily. *Nat. Rev. Immunol.* 2:116–126. https://doi.org/10.1038/nri727

Shrestha, S., K. Yang, C. Guy, P. Vogel, G. Neale, and H. Chi. 2015. Treg cells require the phosphatase PTEN to restrain TH1 and TFH cell responses. *Nat. Immunol.* 16:178–187. https://doi.org/10.1038/ni.3076

Stamper, C.C., Y. Zhang, J.F. Tobin, D.V. Erbe, S. Ikemizu, S.J. Davis, M.L. Stahl, J. Seehra, W.S. Somers, and L. Mosyak. 2001. Crystal structure of the B7-1/CTLA-4 complex that inhibits human immune responses. *Nature*. 410:608–611. https://doi.org/10.1038/35069118

Sun, I.H., A.E. Qualls, H.S. Yin, J. Wang, M.P. Arvedson, J. Germino, N.K. Horner, S. Zhong, J. Du, M. Valdearcos, et al. 2025. RORgammat eTACs mediate oral tolerance and Treg induction. *J. Exp. Med.* 222:e20250573. https://doi.org/10.1084/jem.20250573

Tang, Q., K.J. Henriksen, E.K. Boden, A.J. Tooley, J. Ye, S.K. Subudhi, X.X. Zheng, T.B. Strom, and J.A. Bluestone. 2003. Cutting edge: CD28 controls peripheral homeostasis of CD4+CD25+ regulatory T cells. *J. Immunol.* 171:3348–3352. https://doi.org/10.4049/jimmunol.171.7.3348

Teng, F., R. Tacho-Pinot, B. Sung, D.L. Farber, S. Worgall, H. Hammad, B.N. Lambrecht, M.R. Hepworth, and G.F. Sonnenberg. 2021. ILC3s control airway inflammation by limiting T cell responses to allergens and microbes. *Cell Rep.* 37:110051. https://doi.org/10.1016/j.celrep.2021.110051

Tivol, E.A., F. Borriello, A.N. Schweitzer, W.P. Lynch, J.A. Bluestone, and A.H. Sharpe. 1995. Loss of CTLA-4 leads to massive lymphoproliferation and fatal multiorgan tissue destruction, revealing a critical negative regulatory role of CTLA-4. *Immunity*. 3:541–547. https://doi.org/10.1016/1074-7613(95)90125-6

Viglietta, V., K. Bourcier, G.J. Buckle, B. Healy, H.L. Weiner, D.A. Hafler, S. Egorova, C.R. Guttmann, J.R. Rusche, and S.J. Khoury. 2008. CTLA4Ig treatment in patients with multiple sclerosis: An open-label, phase 1 clinical trial. *Neurology*. 71:917–924. https://doi.org/10.1212/01.wnl.0000325915.00112.61

Walunas, T.L., C.Y. Bakker, and J.A. Bluestone. 1996. CTLA-4 ligation blocks CD28-dependent T cell activation. *J. Exp. Med.* 183:2541–2550. https://doi.org/10.1084/jem.183.6.2541

Walunas, T.L., D.J. Lenschow, C.Y. Bakker, P.S. Linsley, G.J. Freeman, J.M. Green, C.B. Thompson, and J.A. Bluestone. 1994. CTLA-4 can function as a negative regulator of T cell activation. *Immunity*. 1:405–413. https://doi.org/10.1016/1074-7613(94)90071-x

Wang, J., C.A. Lareau, J.L. Bautista, A.R. Gupta, K. Sandor, J. Germino, Y. Yin, M.P. Arvedson, G.C. Reeder, N.T. Cramer, et al. 2021. Single-cell multiomics defines tolerogenic extrathymic Aire-expressing populations with unique homology to thymic epithelium. *Sci. Immunol.* 6:eabl5053. https://doi.org/10.1126/sciimmunol.abl5053

Watanabe, M., C. Fujihara, A.J. Radtke, Y.J. Chiang, S. Bhatia, R.N. Germain, and R.J. Hodes. 2017. Co-stimulatory function in primary germinal center responses: CD40 and B7 are required on distinct antigen-presenting cells. *J. Exp. Med.* 214:2795–2810. https://doi.org/10.1084/jem.20161955

Wheaton, J.D., C.H. Yeh, and M. Ciofani. 2017. Cutting edge: c-Maf is required for regulatory T cells to adopt RORgammat(+) and follicular phenotypes. *J. Immunol.* 199:3931–3936. https://doi.org/10.4049/jimmunol.1701134

Wing, K., Y. Onishi, P. Prieto-Martin, T. Yamaguchi, M. Miyara, Z. Fehervari, T. Nomura, and S. Sakaguchi. 2008. CTLA-4 control over Foxp3+ regulatory T cell function. *Science*. 322:271–275. https://doi.org/10.1126/science.1160062

Xu, M., M. Pokrovskii, Y. Ding, R. Yi, C. Au, O.J. Harrison, C. Galan, Y. Belkaid, R. Bonneau, and D.R. Littman. 2018. c-MAF-dependent regulatory T cells mediate immunological tolerance to a gut pathobiont. *Nature*. 554:373–377. https://doi.org/10.1038/nature25500

Yamano, T., J. Dobes, M. Voboril, M. Steinert, T. Brabec, N. Zietara, M. Dobesova, C. Ohnmacht, M. Laan, P. Peterson, et al. 2019. Aire-expressing ILC3-like cells in the lymph node display potent APC features. *J. Exp. Med.* 216:1027–1037. https://doi.org/10.1084/jem.20181430

Yang, B.H., S. Hagemann, P. Mamareli, U. Lauer, U. Hoffmann, M. Beckstette, L. Fohse, I. Prinz, J. Pezoldt, S. Suerbaum, et al. 2016. Foxp3(+) T cells expressing RORgammat represent a stable regulatory T-cell effector lineage with enhanced suppressive capacity during intestinal inflammation. *Mucosal Immunol.* 9:444–457. https://doi.org/10.1038/mi.2015.74

Zhang, J., K.V. Salojin, J.X. Gao, M.J. Cameron, I. Bergerot, and T.L. Delovitch. 1999. p38 mitogen-activated protein kinase mediates signal integration of TCR/CD28 costimulation in primary murine T cells. *J. Immunol.* 162:3819–3829.

JEM

Supplemental material

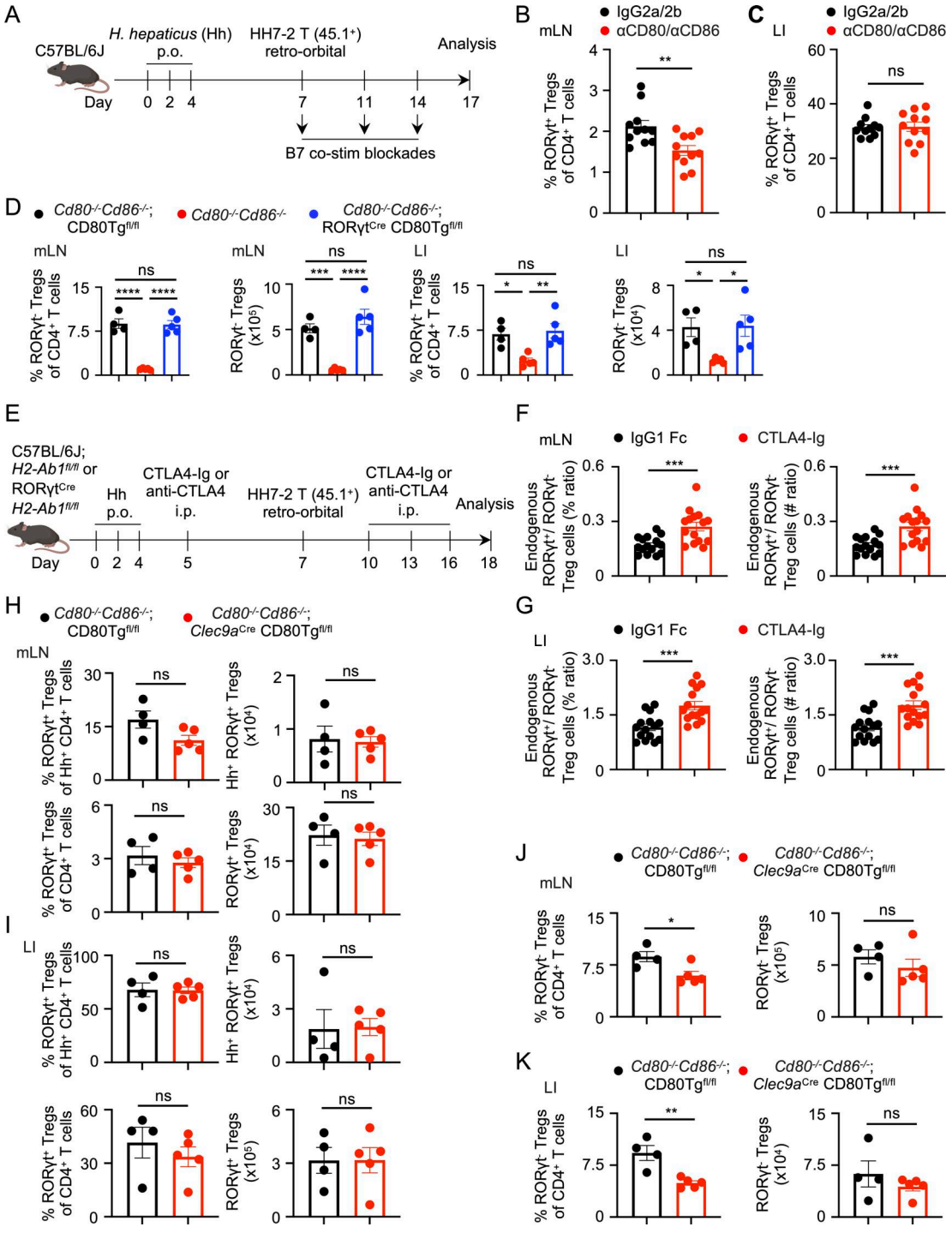

Figure S1. **Experimental designs and immune profiling of RORγt⁺ Treg cells. (A)** C57BL/6J WT mice were colonized with Hh on days 0, 2, and 4, followed by Hh-specific naïve CD4⁺ T cell transfer retro-orbitally on day 7; mice were i.p. injected with blockade of costimulatory molecules B7-1 (CD80) and B7-2 (CD86) on days 7, 11, and 14. Mice were euthanized for analysis on day 17. **(B and C)** Frequency of endogenous CD4⁺ T cells in the (B) mLN and (C) LI of WT mice treated with IgG2a/2b (n = 11) or αCD80/αCD86 (n = 11) as shown in Fig. 1, A–C. **(D)** Frequency and cell number of endogenous RORγt⁻ Treg cells in the mLN (left two panels) and LI (right two panels) of the mice in Fig. 1, D–I. **(E)** C57BL/6J WT or transgenic mice as indicated were orally gavaged with Hh on days 0, 2, and 4, followed by Hh-specific naïve CD4⁺ T cell transfer retro-orbitally on day 7; mice were i.p. injected with CTLA4-Ig or anti-CTLA4 on days 5, 10, 13, and 16. Mice were euthanized for analysis on day 18. **(F and G)** Ratio between endogenous RORγt⁺ and RORγt⁻ Treg cells by frequency (left panels) or cell number (right panels) in the (F) mLN and (G) LI of the mice treated with IgG1 Fc (n = 15) or CTLA4-Ig (n = 15) as shown in Fig. 2, A–C. **(H and I)** Frequencies (left panels in H or I) and cell number (right panels in H or I) of Hh-specific (top panels in H or I) or endogenous (bottom panels in H or I) RORγt⁺ Treg cells in the (H) mLN and (I) LI of *Cd80*$^{-/-}$*Cd86*$^{-/-}$; CD80Tg$^{fl/fl}$ mice (n = 4), and *Clec9a*^{Cre} *Cd80*$^{-/-}$*Cd86*$^{-/-}$; CD80Tg$^{fl/fl}$ mice (n = 5). **(J and K)** Frequency (left panel) and cell number (right panel) of endogenous RORγt⁻ Treg cells in the (J) mLN and (K) LI of the mice in Fig. S1, H and I. The data in Fig. S1 are pooled from three independent experiments. The data are shown as means ± SEM; the statistics shown in B, C, F, G, H, I, J, and K were obtained by unpaired Student's t test (two-tailed); the statistics shown in D were obtained by ordinary one-way ANOVA with Tukey's multiple comparisons test. ns, not significant; *P < 0.05; **P < 0.01; ***P < 0.001; ****P < 0.0001.

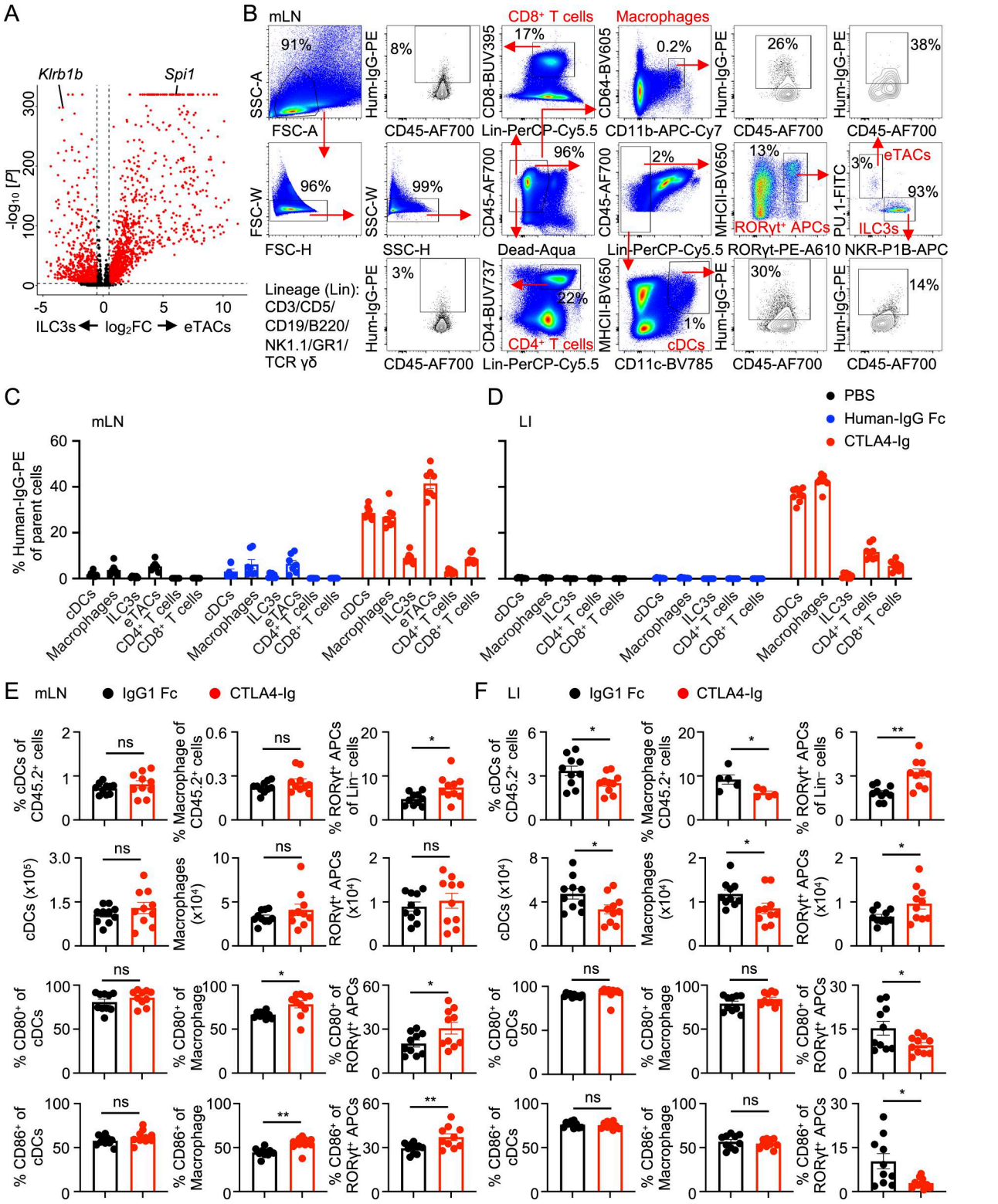

Figure S2. **Flow cytometry gating strategies and profiling of APC subsets and T cells. (A)** Volcano plot showing *Klrb1b* and *Spi1* as differentially expressed genes in LTi-like ILC3s and eTACs, respectively, of the scRNA-seq dataset generated from the healthy mouse mLN samples as published (Lyu et al., 2022). FC, fold change. **(B)** Flow cytometry gating strategies for T cell subsets (CD4⁺ and CD8⁺) and APC populations, including cDCs, macrophages, and RORγt⁺ APCs (eTACs and ILC3s) in the mLN; similar strategies were applied for gating T cells and APC populations in the LI. **(C and D)** Quantification of CTLA4-Ig binding to APC and T cell subsets in the cells isolated from the (C) mLN or (D) LI of the mice followed by incubation with PBS (n = 7), IgG1 Fc (n = 7), and CTLA4-Ig (n = 8). **(E and F)** Frequencies of total, CD80⁺, CD86⁺, or cell numbers of cDCs, macrophages, or RORγt⁺ APCs in the (E) mLN and (F) LI of mice treated with IgG1 Fc (n = 10) and CTLA4-Ig (n = 10). The data in Fig. S2 are pooled from two independent experiments. The data are shown as means ± SEM; the statistics shown in E and F were obtained by unpaired Student's t test (two-tailed). ns, not significant; *P < 0.05; **P < 0.01. cDCs, conventional dendritic cells.

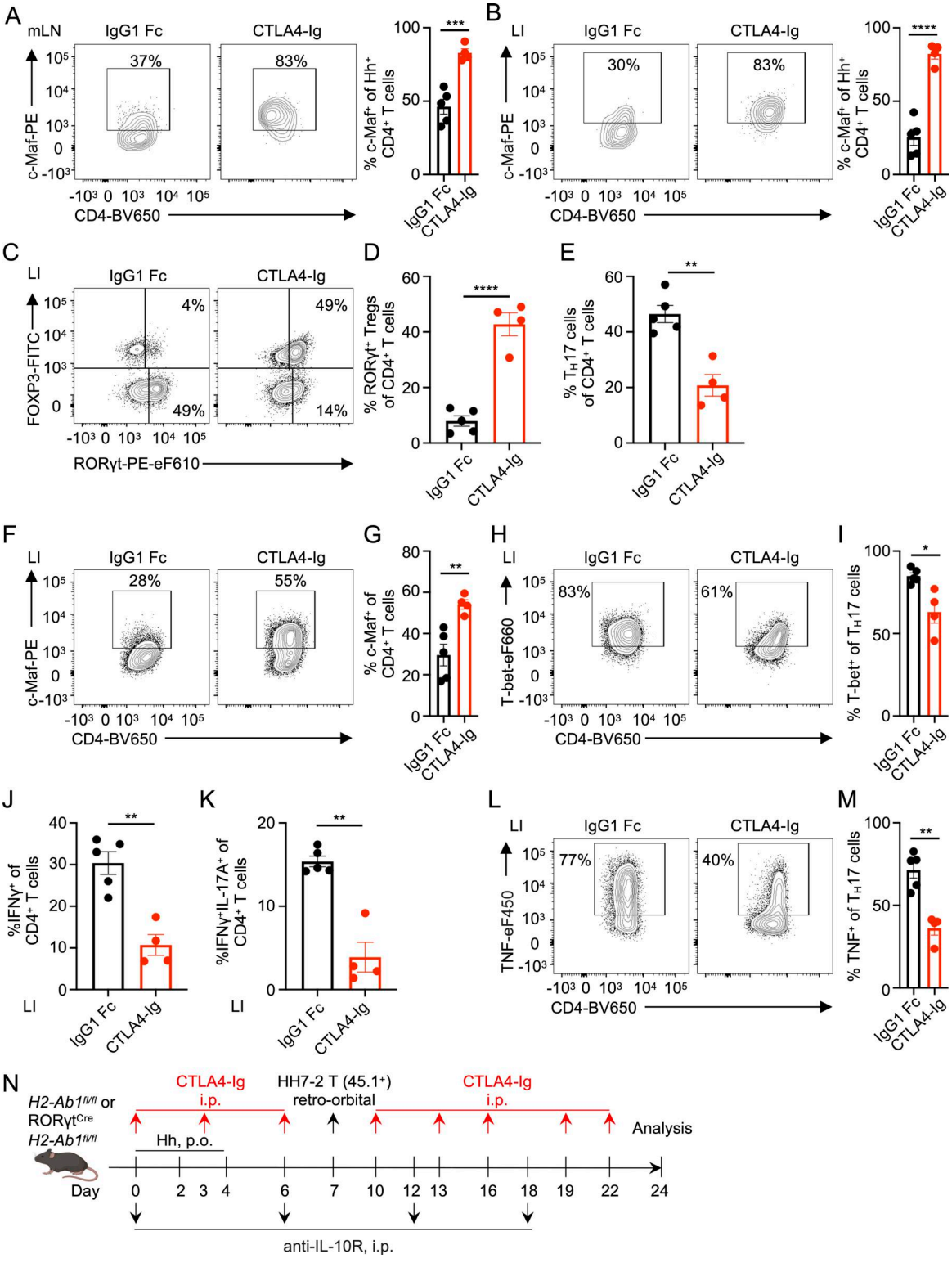

Figure S3. **CTLA4-Ig drives immune regulation in a mouse model of gut inflammation. (A and B)** Flow cytometry plots and frequency of c-Maf$^+$ Hh-specific CD4$^+$ T cells in the (A) mLN and (B) LI of C57BL/6J WT mice treated with IgG1 Fc (n = 5) or CTLA4-Ig (n = 4) as shown in Fig. 3. **(C–G)** (C) Flow cytometry plots and frequencies of endogenous CD4$^+$ T cells in the LI of the mice in Fig. 3, showing (D) RORγt$^+$ Treg cells, (E) T_H17 cells, and (F and G) c-Maf$^+$ cells. **(H–M)** Flow cytometry plots and frequencies of inflammatory endogenous CD4$^+$ T cell subsets in the LI of the mice as shown in Fig. 3, showing (H and I) T-bet$^+$ T_H17 cells, (J) IFNγ$^+$ CD4$^+$ T cells, (K) IFNγ$^+$IL-17A$^+$ CD4$^+$ T cells, and (L, M) TNF$^+$ T_H17 cells. **(N)** *H2-Ab1*$^{fl/fl}$ mice and RORγt^{Cre} *H2-Ab1*$^{fl/fl}$ mice were colonized with Hh on days 0, 2, and 4, followed by Hh-specific naïve CD4$^+$ T cell transfer retro-orbitally on day 7; mice were i.p. injected with anti-IL-10R on days 0, 6, 12, and 18, and were i.p. injected with CTLA4-Ig on days 0, 3, 6, 10, 13, 16, 19, and 22. Mice were euthanized for analysis on day 24. The data in Fig. S3 are representative of two independent experiments. The data are shown as means ± SEM; the statistics shown in A, B, D, E, G, I, J, K, and M were obtained by unpaired Student's t test (two-tailed). *P < 0.05; **P < 0.01; ***P < 0.001; ****P < 0.0001.